The role of the spin and orbital components of the nuclear current in forming multipole resonances of light nuclei

N. G. Goncharova
Nuclear Physics Institute, Moscow State University

Fiz. Élem. Chastits At. Yadra **29**, 789–831 (July–August 1998)

A microscopic analysis is performed of the contributions of the orbital and spin currents to multipole $1\hbar\omega$ resonances in the (e,e') cross sections of excitations of $1p$- and $1d-2s$-shell nuclei. The dependence of the transverse form factors and their spin and orbital components on the momentum transferred to the nucleus is traced for all single-particle transitions. Effects of the destructive interference of the spin and orbital components are revealed for several transitions from the $1p$ and $1d-2s$ shells. A method is proposed for determining the configurational structure of the wave functions of multipole excited states. The dependence of the weighted mean energies of $E1$ and $M2$ resonances in the (e,e') cross sections on the momentum transfer is interpreted as the result of the interplay of the orbital, spin-dipole, and spin-octupole modes in multipole excitations of light nuclei. © *1998 American Institute of Physics.* [S1063-7796(98)00104-1]

1. INTRODUCTION

In the last 15–20 years the amount of experimental data on nuclear structure and nuclear excitations in reactions involving various probes has grown rapidly, owing to accelerator experiments at intermediate energies, and this has posed a number of serious problems for nuclear theory. One is the adequate interpretation of the data obtained in a rather large range of momentum transfers q, where the total nuclear excitation cross section is composed of the contributions of resonances of various multipole orders. Even for light nuclei, where the number of doorway states is relatively small, it is quite difficult to separate the contributions of individual multipole resonances (MRs). An even more complicated problem is the identification of the transitions forming MRs. One method of determining the quantum numbers of a transition and the role of the various nuclear degrees of freedom in forming the excitation function is analysis of the form factors for electroexcitation of MRs.

As a probe in nuclear-structure studies, the electron has a number of advantages over other particle probes:

1. The amplitude of the electromagnetic interaction, in contrast to the strong and weak interactions, is known accurately from quantum-electrodynamical calculations, and so no model assumptions about the interaction Hamiltonian are needed.

2. The electromagnetic nature of the interaction between an electron and a nucleus greatly simplifies the interpretation of the experimental results compared to the case of hadron scattering, because in (e,e') reactions there are no significant changes in the structure of the nuclear target, and first-order perturbation theory is adequate, owing to the smallness of the electromagnetic interaction constant.

3. There is no problem with separating effects of the probe–target-nucleus interaction from effects directly related to the structure of the target itself.

4. Although all the advantages mentioned above are also valid for photonuclear reactions, a particular advantage of (e,e') reactions is that in electron interactions with a nucleus the momentum transfer q can be varied, whereas in the scattering of real γ quanta the momentum transferred to the nucleus is equal to the γ energy ω, which, when recoil is neglected, is the nuclear excitation energy (here and below we use the natural system of units where $\hbar=c=1$; $1\ \mathrm{F}^{-1}\approx 198$ MeV). The possibility of varying the momentum transfer opens up broad vistas in the study of nuclear structure and excited states of nuclei. During the first stage of studying nuclei using electromagnetic interactions, the experimental data on electron elastic scattering ($\omega=0$) at various momentum transfers served as the principal source of information about the charge density distributions and the magnetization current in ground-state nuclei. Later on, the new experimental possibilities which arose when both q and ω are varied allowed the separation and detailed study of the location and structure of nuclear excitations of various multipole orders. Finally, the appearance of a new generation of intermediate-energy electron accelerators with large average current and D-factor of nearly 100%, and also the use of improved spectrometers, began a new stage of nuclear studies based on (e,e') reactions. This also significantly broadened the range of phenomena which could be studied and raised the reliability of the experimental data. Increase of the momentum transferred to the nucleus to about $3\ \mathrm{F}^{-1}$ at energies $\omega\leqslant 35$ MeV involves resonances of higher multipole orders in the excitation.

The multipole order of a resonance excitation is usually identified by studying the dependence of the form factor on the momentum transferred to the nucleus. However, the q dependences of the form factors of MRs of different multipole orders are similar for some transitions. The dependence of the MR form factors on the momentum transfer depends strongly on the quantum numbers of the transitions dominating in the excited-state wave function. The matrix elements

of the electron interaction with the intranuclear current play the leading role in forming the nuclear response functions in large-angle electron scattering. The main components of the nuclear current are the nucleon convection current and the spin magnetization current. The interference of these components for various q also determines the cross section for large-angle electron scattering. The relative importance of the orbital and spin components of the nucleon intranuclear current in the cross section for electroexcitation of MRs strongly depends on the momentum transferred to the nucleus. At relatively large momentum transfers ($q > 1\,\mathrm{F}^{-1}$) and large scattering angles, the dominant contribution to the cross section for MR excitation comes from the spin components of the nucleon intranuclear current, which exists because the nucleon possesses a magnetic moment. Meanwhile, at small q convection (orbital) excitation modes associated with the charge distribution and the convection current in the nucleus play an important role in forming the transverse component of the nuclear response function. This general trend in the interplay of the contributions of the spin and orbital components of the nucleon intranuclear current also involves the individual features associated with the quantum numbers of the transitions dominating in MR formation. It is therefore essential to perform a detailed analysis of the factors affecting the formation of the function describing the nuclear response to a multipole excitation. At the level of the nucleon degrees of freedom this implies separation of the contribution of the intranuclear convection current and the magnetization current, and understanding the relative role of each for various kinematical reaction parameters. Since the nuclear magnetization current, in contrast to the convection current, is directly related to the spin component of the nucleon current, a microscopic analysis of the structure of the nuclear excitations can separate the spin-multipole excitation modes from the convection ones. Whereas the latter have been the subject of intense study for many years now, particularly for the giant dipole ($E1$) resonance in photonuclear reactions, interest in the spin modes has arisen only recently, owing to the new possibilities of studying nuclear multipole excitations at large momentum transfers.

The present study is devoted to a microscopic analysis of the contributions of the spin and orbital components of the nucleon current to $1\hbar\omega$ excitations of multipole resonances of light nuclei. The excitation spectra of light nuclei give the clearest manifestation of the properties of the single-particle transitions contributing to multipole excitations, while the features of the microscopic structure in the spectra of heavier nuclei are usually suppressed by collective effects, making it difficult to check the ability of various models to describe the experimental picture.

Here we analyze the specific manifestations of the contributions of the spin and orbital currents to resonances of various multipole orders for the example of electroexcitation reactions. Restricting ourselves to only this one type of nuclear reaction does not make the analysis less general, because the spin–angular dependence of the one-particle operators responsible for multipole excitations is universal for many nuclear reactions.

The contributions of spin and orbital excitation modes to multipole resonances of specific nuclei can be studied only by using model representations. Here we use the matrix elements of multipole operators obtained in the multiparticle shell model, which is a systematic method for microscopically describing internal nuclear excitation modes. The wave functions of excited states of $1p$- and $1d-2s$-shell nuclei are calculated using the "particle–state of the final nucleus" "particle–core coupling" (PCC) version of the multiparticle shell model, which allows the inclusion of the distribution of hole configurations over states of nuclei $(A-1)$ genetically related to the ground state of the nucleus A.

2. STRUCTURE OF THE ELECTROEXCITATION FORM FACTORS

The inclusive differential cross section for electron scattering on a nucleus is related to the nuclear form factors as[1–3]

$$\frac{d^2\sigma}{d\Omega d\omega} = \frac{Z^2\sigma_M}{\eta_R}\left\{\left(\frac{q_\mu^4}{q^4}\right)F_L^2(q,\omega)+\left(\frac{1}{2}\left(\frac{q_\mu^2}{q^2}\right)+\tan^2\left(\frac{\Theta}{2}\right)\right)F_T^2(q,\omega)\right\}. \tag{2.1}$$

Here Θ is the electron scattering angle, $\sigma_M = \alpha^2\cos^2(\Theta/2)/4\varepsilon_1^2\sin^4(\Theta/2)$ is the cross section for electron scattering on a structureless charge (the Mott cross section), ε_1 is the energy of the primary electron beam, $\eta_R = 1 + (2\varepsilon_1\sin^2(\Theta/2)/M_T)$ is the recoil factor, M_T is the target mass, and $q_\mu^2 = q^2 - \omega^2$ ($q = k_f - k_i \approx 2\varepsilon_1\sin(\Theta/2)$ is the momentum transfer). Using the fact that, as a rule, in (e,e') reactions $q \gg \omega$ and so $q_\mu^2 \approx q^2$, Eq. (2.1) can be written as

$$\frac{d^2\sigma}{d\Omega d\omega} = \frac{Z^2\sigma_M}{\eta_R}\left\{F_L^2(q,\omega)+\left(\frac{1}{2}+\tan^2\left(\frac{\Theta}{2}\right)\right)F_T^2(q,\omega)\right\}. \tag{2.2}$$

For inclusive cross sections, all the information about the nuclear structure is concentrated in the longitudinal (Coulomb) and transverse form factors F_L^2 and F_T^2. These are respectively related to the charge density and the nuclear current density through the matrix elements of multipole operators $\hat{M}_J^{\mathrm{Coul}}$ and $\hat{T}_J^{\mathrm{el}}$, $\hat{T}_J^{\mathrm{mag}}$:

$$F_L^2 = \frac{4\pi}{Z^2}(2J_i+1)^{-1}\sum_J |\langle J_f\|\hat{M}_J^{\mathrm{Coul}}\|J_i\rangle|^2, \tag{2.3}$$

$$F_T^2 = \frac{4\pi}{Z^2}(2J_i+1)^{-1}\sum_J \{|\langle J_f\|\hat{T}_J^{\mathrm{el}}\|J_i\rangle|^2 + |\langle J_f\|\hat{T}_J^{\mathrm{mag}}\|J_i\rangle|^2\}, \tag{2.4}$$

where J_i and J_f are the nuclear spins in the initial and final states,

$$\hat{M}_{JM}^{\mathrm{Coul}}(q) = \int d^3r j_J(qr)Y_{JM}(\Omega)\rho(r) \tag{2.5}$$

is the multipole Coulomb operator, and

$$\hat{T}_{JM}^{\mathrm{el}}(q) = \frac{1}{q}\int d^3r[\hat{\nabla} j_J(qr)]Y_{JJ1}^M(\Omega)J(r), \tag{2.6}$$

$$\hat{T}^{\text{mag}}_{JM}(q)=\int d^3r j_J(qr)Y^M_{JJ1}(\Omega)J(r). \tag{2.7}$$

Here $Y^M_{JJ1}=\Sigma\langle Jm1m'|JM\rangle Y_{JM}\bar{e}_{m'}$ are the vector spherical harmonics, $j_J(qr)$ are the spherical Bessel functions, $\rho(r)$ is the charge-density operator, and $J(r)$ is the nuclear-current density operator, which contains the contributions of the convection (orbital) current, the spin current (magnetization current), and the currents associated with excitations of non-nucleon degrees of freedom in the nucleus. In this range of excitation energies and momentum transfers ($E\leqslant 35$ MeV and $q\leqslant 2.5$ F^{-1}) non-nucleon degrees of freedom are manifested mainly as meson exchange currents (MECs). The results of theoretical calculations of the form factors of multipole resonances discussed here are obtained by neglecting the MEC contributions.

The longitudinal (Coulomb) form factor F^2_L can be represented as the sum over J of multipole form factors F^2_{CJ}:

$$F^2_L(q)=\sum_J F^2_{CJ}(q). \tag{2.8}$$

The transverse form factor $F^2_T(q)$ is the sum of the multipole form factors of electric (EJ) and magnetic (MJ) transitions:

$$F^2_T(q)=\sum_J \{F^2_{EJ}(q)+F^2_{MJ}(q)\}. \tag{2.9}$$

The electric and magnetic form factors do not interfere with each other, because the corresponding multipole operators have opposite parities. There are two ways of separating the contributions of the longitudinal and transverse form factors to the inclusive cross section for (e,e') scattering: by studying the dependence of the cross section on Θ for fixed q and ω [see (2.2)] (the Rosenbluth method), and by measuring the cross section at $\Theta=180°$, where the contribution of the longitudinal form factor is zero:

$$\left.\frac{d^2\sigma}{d\Omega d\omega}\right|_{\Theta=180°}=\frac{Z^2\alpha^2}{4\varepsilon_1^2}\left(1+\frac{2\varepsilon_1}{M_T}\right)^{-1}F^2_T(q,\omega). \tag{2.10}$$

It is also necessary to include the fact that the operators (2.5)–(2.7) act not only in configuration but also in isospin space, where in the latter they are the sum of an isoscalar and an isovector. Taking into account the reduction in the isospin T, the expression for the multipole form factors takes the form

$$F^2_{KJ}=\frac{4\pi}{Z^2}(2J_i+1)^{-1}(2T_f+1)^{-1}|\langle T_iM_{T_i}T0|T_fM_{T_f}\rangle|^2\left|\left\langle J_fT_f\left\|\sum\hat{B}_{JT}\right\|J_iT_i\right\rangle\right|^2, \tag{2.11}$$

where K corresponds to E or M. At low energies of the primary beam and small scattering angles, when $q\approx\omega$, (e,e') scattering experiments give practically the same information as photonuclear reactions. For photonuclear reactions $q^2_\mu=0$, and the absorption cross section is related only to the transverse form factor at the point $q=\omega$:

$$\int\sigma d\omega=\frac{Z^2 2\pi\alpha}{\omega}F^2_T(q=\omega), \tag{2.12}$$

where $\int\sigma d\omega$ is the absorption cross section integrated over the resonance. In the pointlike-nucleon approximation the matrix elements of the multipole operators (2.5)–(2.7) are linear combinations of single-particle operators constructed from the spin operator $\hat{\sigma}$, the angular-momentum operator $\hat{\nabla}$, and the spherical harmonics Y_{JM}:

$$\hat{M}^{\text{Coul}}_{JM}=\sum_{i=1}^{A}\hat{e}_i j_J(r_i)Y_{JM}(\Omega_1), \tag{2.13}$$

$$\hat{T}^{\text{el}}_{JM}=\frac{q}{2M}\sum_{i=1}^{A}\left\{\hat{g}_i j_J(qr_i)[Y_J(Q_i)\times\hat{\sigma}_i]_{JM}+\frac{2\hat{e}_i}{q}\left(\sqrt{\frac{J+1}{2J+1}}\,j_{J-1}(qr_i)[Y_{J-1}(\Omega_i)\times\hat{\nabla}_i]_{JM}-\sqrt{\frac{J}{J+1}}\,j_{J+1}(qr_i)[Y_{J+1}(\Omega_i)\times\hat{\nabla}_i]_{JM}\right)\right\}, \tag{2.14}$$

$$\hat{T}^{\text{mag}}_{JM}=\frac{iq}{2M}\sum_{i=1}^{A}\left\{\hat{g}_i\left(\sqrt{\frac{J+1}{2J+1}}\,j_{J-1}(qr_i)[Y_{J-1}(\Omega_i)\times\hat{\sigma}_i]_{JM}-\sqrt{\frac{J}{2J+1}}\,j_{J+1}(qr_i)[Y_{J+1}(\Omega_i)\times\hat{\sigma}_i]_{JM}\right)-\frac{2\hat{e}_i}{q}j_J(qr_i)[Y_J(\Omega_i)\times\hat{\nabla}_i]_{JM}\right\}. \tag{2.15}$$

Here M is the nucleon mass, and $\hat{e}_i$ and $\hat{g}_i$ are the charge and magnetic-moment operators in isospin space:

$$\hat{e}_i=e_0+e_1\hat{\tau}_{3i}, \tag{2.16}$$

$$\hat{g}_i=\frac{g_p+g_n}{2}+\frac{g_p-g_n}{2}\hat{\tau}_{3i}, \tag{2.17}$$

where g_p and g_n are the proton and neutron magnetic moments in nuclear magnetons. The magnetic moments of unbound nucleons are used in most calculations. The effect on the calculated form factors of using the "renormalized" values of the magnetic moments, equal to $g=0.7$ times the unrenormalized values, will be discussed below. The finite size of the nucleon, which must be included when using Eqs. (2.13)–(2.15), is taken into account by introducing the form factor f_{SN} into the right-hand side of (2.11) (Ref. 2):

$$f_{SN}=\left(1+\frac{q^2}{q_N^2}\right)^{-1};\quad q_N=855\ \text{MeV}. \tag{2.18}$$

In the $1p$-shell calculations we also used the expression for f_{SN} from Ref. 4:

$$f_{SN}(q)=\frac{0.312}{1+q^2/6.0}+\frac{1.312}{1+q^2/15.02}-\frac{0.709}{1+q^2/44.08}$$

$$+\frac{0.085}{1+q^2/154.2}. \qquad (2.18')$$

At momentum transfers q less than 2.0 F^{-1} the two versions of including the finite size of the nucleon lead to similar values of the MR form factors. The correction associated with the motion of the nuclear center of mass, which also must be introduced into the right-hand side of (2.11), has the following form when the harmonic-oscillator approximation is used for the wave functions (HOWFs):[1]

$$f_{\rm cm}(q)=\exp\left[\frac{1}{A}\left(\frac{qb}{2}\right)^2\right], \qquad (2.19)$$

where b is the oscillator parameter. The above formalism for calculating the multipole form factors was constructed in the PWBA, and so it does not include the effect of distortion of the electron waves in the Coulomb field of the nucleus. However, for nuclei with small Z the distortions are small, and they can be approximately included by comparing the results of the PWBA calculation with the experimental points shifted upward along the q axis. These points are therefore functions of $q_{\rm eff}$, which is related to q as[5]

$$q_{\rm eff}=q\left[1+f(q)\left(\frac{Ze^2}{2\varepsilon_1 R}\right)\right], \qquad (2.20)$$

where R is the radius of a sphere equivalent to the target nucleus and $f(q)$ is an empirically selected function of the momentum transfer q.

Equations (2.13)–(2.15) represent spin–angular operators of three types: $Y_{JM}(\Omega)$ corresponds to the interaction of the test particle with the charge,

$$[Y_L\times\hat{\nabla}]_{JM}=\sum\langle LM1\Lambda|JM\rangle Y_{LM}\hat{\nabla}_\Lambda \qquad (2.21)$$

corresponds to the interaction with the convection current, and

$$[Y_L\times\hat{\sigma}]_{JM}=\sum\langle LM1\Lambda|JM\rangle Y_{LM}\hat{\sigma}_N \qquad (2.22)$$

corresponds to the interaction with the spin current. It is useful to separate the spin–angular and radial variables because the spin and angular dependences of the matrix elements of single-particle operators are universal for the electromagnetic, strong, and weak interactions, while the radial dependence is determined by the dynamics of a particular reaction.[6,7]

Analysis of Eqs. (2.14) and (2.15) shows that the relative contribution of the spin modes $j_L(qr)[Y_L\times\hat{\sigma}]_{JM}$ to both the MJ and the EJ form factors grows with increasing q. If in the long-wavelength limit ($q\approx 0$) the q dependences of the longitudinal and transverse electric form factors are coupled (the Siegert theorem),

$$F_{EJ}|_{q=0}=\frac{\omega}{q}\sqrt{\frac{J+1}{J}}F_{CJ}, \qquad (2.23)$$

then at higher q, when spin modes start to become important in the excitation of EJ multipoles, the CJ and EJ form factors begin to behave quite differently from each other.

It also follows from (2.14) and (2.15) that only the spin operator $j_J(qr)[Y_J\times\hat{\sigma}]_{JM}$ is involved in forming EJ resonances, while the spin modes of MJ transitions are due to two types of spin operator: $j_{J-1}(qr)[Y_{J-1}\times\hat{\sigma}]_{JM}$ and $j_{J+1}(qr)[Y_{J+1}\times\hat{\sigma}]_{JM}$. The exception is transitions with the maximum allowed value of the spin $MJ_{\rm max}$. The spin operator $j_{J+1}(qr)[Y_{J+1}\times\hat{\sigma}]_{JM}$ does not contribute to their excitation, nor does the convection current. Therefore, $MJ_{\rm max}$ transitions ($M4$ for $1p$-shell nuclei and $M6$ for $1d-2s$-shell nuclei) are due only to the spin operator $j_{J-1}(qr)[Y_{J-1}\times\hat{\sigma}]_{JM}$. The same spin–angular operator also dominates in the excitation of these transitions in hadron scattering reactions, which makes it possible to perform a combined spectroscopic analysis of the results of (e,e'), (π,π'), and (N,N') experiments.[8,9]

Since the form of the spin–angular single-particle operators generating a multipole excitation is independent of the interaction dynamics, it is convenient to separate the matrix elements of single-particle operators from the spectroscopic features of the states of specific nuclei. The multipole operators $\hat{T}_J^{\rm el}$ and $\hat{T}_J^{\rm mag}$ are linear combinations of products of operators depending on the spatial and spin–angular variables and the isospin operator:

$$\hat{B}_{JM}=\sum\hat{O}_{JM,TM}(i)\hat{\tau}_{TM}(i). \qquad (2.24)$$

where $\hat{O}$ is a tensor operator of rank J and $\hat{\tau}_T$ are operators in isospin space. A characteristic of the nuclear response to an excitation is the multipole spectroscopic amplitude:[6]

$$Z_{J,TM}(j_fj_i)=(2J+1)^{1/2}(2J_i+1)^{-1/2}\langle J_fT_fM_T\|[\hat{a}_f^+\hat{a}_i],\|J_iT_iM_T\rangle, \qquad (2.25)$$

where $\hat{a}^+$ and $\hat{a}$ are creation and annihilation operators.

Obtaining an adequate microscopic descripton of nuclear ground and excited states is one of the most complicated problems in theoretical nuclear physics. Approximation methods based on the particle–hole version of the multiparticle shell model give satisfactory results for light and intermediate nuclei close to magic nuclei. One version of the shell model is an approach which allows the distribution of hole states over levels of the final nucleus to be taken into account. It was proposed in Ref. 10 and used to calculate the excited-state wave functions for nuclei with from 7 to 15 nucleons, including nuclei with ground states very far from filled-shell states.[11–17] In what follows we shall refer to this version of the multiparticle shell model, which for a nucleus with A nucleons involves the introduction of basis configurations constructed in the form of a product of nucleon and final-nucleus $(A-1)$ wave functions, as the PCC (particle–core coupling) model. The results for the form factors of specific nuclei given below were mainly obtained using the PCC version of the multiparticle shell model for multipole resonances corresponding to $1\hbar\omega$ excitations. In the PCC representation the spectroscopic amplitude has the form

$$Z_{J,T}(j'j)=(2T+1)^{1/2}(2T_i+1)^{1/2}(2J_f$$

$$+1)^{1/2}\langle T_i M_{T,} TM_T | T_f M_{T_f}\rangle N \sum \alpha_f^{J'j'} C_i^{J'j}$$

$$(-1)^k W(J_i J_f jj'; JJ') W\left(T_i T_f \frac{1}{2}\frac{1}{2}; TT'\right), \tag{2.26}$$

where N is the number of nucleons in the shell, $\alpha_f^{J'j'}$ are the coefficients of the expansion of the excited-state wave functions in basis configurations, $C_i^{J'j}$ are the fractional-parentage coefficients for the ground state of the target nucleus, and $k=J'+j_f-J_i-J+T'-T_i+\frac{1}{2}-T$.

The reduced matrix element of the operator (2.24) in the space of nuclear wave functions can be expressed in terms of the spectroscopic amplitudes and matrix elements of single-particle operators in the space of nucleon wave functions:

$$\langle J_f T_f \| \hat{B}_{JT} \| J_i T_i\rangle = \sum \langle j_f \| \hat{O}_J(i) \| J_i\rangle \sqrt{(2J_f+1)} Z_{J,T}. \tag{2.27}$$

In the HOWF approximation the matrix elements of multipole operators (2.5)–(2.7) have the form[3]

$$\langle j_f \| \hat{M}_{JT}^{\text{Coul}} \| j_i\rangle = \left(\frac{3}{4\pi}\right)^{1/2}\left(1+\frac{q^2}{8M^2}\right) \times (1-2g_v) y^{J/2} e^{-y} P_{CJ}(y); \tag{2.28}$$

$$\langle j_f \| \hat{M}_{JT}^{\text{el}} \| j_i\rangle = \left(\frac{3}{4\pi}\right)^{1/2}\left(\frac{1}{bM}\right) y^{(J-1)/2} e^{-y} P_{EJ}(y); \tag{2.29}$$

$$\langle j_f \| \hat{M}_{JT}^{\text{mag}} \| j_i\rangle = \left(\frac{3}{4\pi}\right)^{1/2}\left(\frac{1}{bM}\right) y^{J/2} e^{-y} P_{MJ}(y), \tag{2.30}$$

where $y=(qb/2)^2$. The explicit form of the polynomials $P(y)$ for $1\hbar\omega$ transitions in $1p$-shell nuclei is given in Table I, which reveals some characteristic features of the form factors of $1\hbar\omega$ excitations. In particular, all transverse multipole form factors, except for $M4$ excitations, contain contributions from both spin operators and operators associated with the convection current. Here the spin-dipole $j_1(qr)[Y_1 \times \hat{\sigma}]_{JM}$ and spin-octupole $j_3(qr)[Y_3 \times \hat{\sigma}]_{JM}$ operators participate in the formation of spin modes of $1\hbar\omega$ excitations of $1p$-shell nuclei. The spin components of $E1$ excitations are generated only by the spin-dipole operator, while $E3$ and $M4$ excitations are generated only by the spin-octupole operators. Both types of spin operator are involved in exciting $M2$ transitions. Since $(g_v/g_s)^2 \approx 29$, mainly isovector ($T_f = T_{i+1}$) nuclear excitations are manifested in (e,e') reactions.

The matrix elements of the form factors of single-particle transitions, the results for which are given below, were calculated using the harmonic-oscillator wave functions (HOWFs). Calculations using more realistic nucleon wave functions obtained for a well of finite depth, for example, the Woods–Saxon potential, lead to the appearance of an additional extremum for $q>3$ F^{-1}, and also to an effective decrease of the form factors.[18,19] However, for $q<2.5$ F^{-1} the experimental q dependences of the form factors are described well by the HOWF calculations.

The behavior of the summed form factors of $1\hbar\omega$ transitions for nuclei at the beginning and the end of the p shell is illustrated in Fig. 1 for the example of ^{7}Li and ^{14}N (Ref. 20). The location of the extrema of the summed form factors is practically independent of the specific nucleus, but is determined by the type of operator generating excitations of a given multipole order. For example, the spin-dipole operator $j_1(qr)[Y_1 \times \hat{\sigma}]_{JM}$ dominates in the excitation of $E1$ and $M2$ transitions at $q \approx 1$ F^{-1} (the first maximum of the $M2$ resonance and the spin–isospin $E1$ resonance), as a result of which the summed form factors of these transitions have very similar q dependences in this range of momentum transfers. The same situation occurs for $E3$ and $M4$ transitions due to the spin-octupole operator $j_3(qr)[Y_3 \times \hat{\sigma}]_{JM}$. (It should be noted that the similarity of the q dependences of the EJ and $M(J+1)$ form factors does not prevent them from being distinguished experimentally, because electric multipoles, in contrast to magnetic ones, have longitudinal components CJ.) The spin-octupole operator also plays an important role in forming the second maximum of the form factor of $M2$ excitations, where it acts together with the spin-dipole operator.

The filling of subshells does not noticeably affect the q dependence of the multipole form factors, but is manifested mainly in the ratio of their values. For example, the magnitude of the total form factor for the $M4$ excitation of ^{7}Li exceeds that of the total $E3$ form factor, while the situation is the opposite for both ^{14}N and ^{15}N (Ref. 16). This is because the excitation of $E3$ multipoles, in contrast to $M4$ ones, receives an important contribution from transitions from the $1p_{1/2}$ subshell, the probability of which grows for nuclei at the end of the $1p$ shell.

In Fig. 2 for the example of ^{15}N we show the energy distribution of the multipole form factors for two values of the momentum transfer, $q=0.7$ F^{-1} and $q=1.3$ F^{-1}, from the data of Ref. 16. The PCC calculation includes the decay widths of the resonance states. We clearly see the variation of the relative contributions of states of various multipole orders to the total cross section for backward electron scattering. At momentum transfers of 1.3 F^{-1} and above the contribution of the orbital current to the transverse MR form factors in electroexcitation is practically absent, and the spin components of the nucleon current and the meson exchange currents participate in forming the nuclear response functions. The role played by MECs in forming multipole resonances is not understood. In Ref. 21 the MEC contribution to the $M1$ isovector form factor of ^{28}Si was estimated to be about 25% of the transition strength. The study of the behavior of the transverse form factors near nondiffraction minima, where the contributions of the spin and orbital components of the nucleon current cancel each other out, is one of the most promising methods for explaining the role of non-nucleon degrees of freedom of the nucleus in forming multipole resonances.

3. ELECTRIC DIPOLE EXCITATIONS OF LIGHT NUCLEI

The analysis of the contributions of the spin and orbital components of the intranuclear nucleon current to the

TABLE I. Matrix elements of multipole operators of $1\hbar\omega$ excitations in the $1p$ shell.

$$\left\langle l\frac{1}{2}j\left\|\hat{O}\right\|l'\frac{1}{2}j'\right\rangle=\sqrt{\frac{4\pi}{Z}}\,C_J\langle j\|\hat{O}\|j'\rangle$$

C_J

$\hat{M}_J^{\mathrm{Coul}}$	$\hat{T}_J^{\mathrm{el}}$	$\hat{T}_J^{\mathrm{mag}}$
$\sqrt{\frac{3}{4\pi}}\left(1+\frac{q^2}{8M^2}\right)(1-2g_\nu)y^{\frac{1}{2}}e^{-y}$	$\sqrt{\frac{3}{4\pi}}\frac{1}{bM}y^{(J-1)/2}e^{-y}$	$\sqrt{\frac{3}{4\pi}}\frac{1}{bM}y^{j/2}e^{-y}$

$\langle j\|\hat{O}\|j'\rangle$

	ΔT	$1p_{3/2}$			$1p_{1/2}$		
		$1d_{5/2}$	$1d_{3/2}$	$2s_{1/2}$	$1d_{5/2}$	$1d_{3/2}$	$2s_{1/2}$
$C1$	1	$2\left(1-\frac{2}{5}y\right)$	$-\frac{2}{3}\left(1-\frac{2}{5}y\right)$	$\frac{2\sqrt{2}}{3}(1-y)$		$\frac{2\sqrt{5}}{3}\left(1-\frac{2}{5}y\right)$	$\frac{2}{3}(1-y)$
	0	$\sqrt{\frac{2}{3}}\left(1-\frac{2}{5}\right)$	$-\frac{\sqrt{2}}{3\sqrt{3}}\left(1-\frac{2}{5}\right)$	$\frac{2}{3\sqrt{3}}(1-y)$		$\frac{\sqrt{10}}{3\sqrt{3}}\left(1-\frac{2}{5}y\right)$	$\frac{\sqrt{2}}{3\sqrt{3}}(1-y)$
$E1$	1	$-\sqrt{2}\left[\left(1-\frac{4}{5}y\right)+g_\nu y\left(\frac{2}{5}y-1\right)\right]$	$\frac{\sqrt{2}}{3}\left[\left(1-\frac{4}{5}y\right)+4g_\nu y\left(1-\frac{2}{5}y\right)\right]$	$-\frac{2}{3}[(1+y)+g_\nu y(1-y)]$		$\frac{\sqrt{10}}{3}\left[\left(1-\frac{4}{5}y\right)-g_\nu y\left(1-\frac{2}{5}y\right)\right]$	$\frac{\sqrt{2}}{3}[(1+y)+2g_\nu y(1-y)]$
	0	$-\frac{1}{\sqrt{3}}\left[\left(1-\frac{4}{5}y\right)+g_s y\left(\frac{2}{5}y-1\right)\right]$	$\frac{1}{3\sqrt{3}}\left[\left(1-\frac{4}{5}y\right)+4g_s y\left(1-\frac{2}{5}y\right)\right]$	$\frac{\sqrt{2}}{3\sqrt{3}}[(1+y)+g_s y(1-y)]$		$\frac{5}{3\sqrt{3}}\left[\left(1-\frac{4}{5}y\right)-g_s y\left(1-\frac{2}{5}y\right)\right]$	$\frac{1}{3\sqrt{3}}[(1+y)+2g_s y(1-y)]$
$M2$	1	$-\frac{2\sqrt{70}}{15}\left[1+g_\nu\left(\frac{3}{2}-\frac{5}{7}y\right)\right]$	$\frac{2\sqrt{30}}{15}(1-g_\nu)$	$-\frac{2}{\sqrt{3}}g_\nu(1-y)$	$-\frac{4}{3\sqrt{5}}[1-g_\nu(3-y)]$	$-\frac{2\sqrt{2}}{15}\left[1-g_\nu\left(\frac{1}{2}-y\right)\right]$	
	0	$-\frac{2\sqrt{35}}{15\sqrt{3}}\left[1+g_s\left(\frac{3}{2}-\frac{5}{7}y\right)\right]$	$\frac{2\sqrt{5}}{15}(1-g_s)$	$-\frac{\sqrt{2}}{3}g_s(1-y)$	$-\frac{2\sqrt{2}}{3\sqrt{15}}[1-g_s(3-y)]$	$-\frac{2}{15\sqrt{3}}\left[1-g_s\left(\frac{1}{2}-y\right)\right]$	
$C3$	1	$-\frac{4\sqrt{6}}{15}$	$\frac{4}{5}$		$-\frac{2\sqrt{30}}{15}$		
	0	$-\frac{4}{15}$	$\frac{4}{5\sqrt{6}}$		$-\frac{2\sqrt{5}}{15}$		
$E3$	1	$\frac{4\sqrt{2}}{15}\left(1-\frac{1}{2}g_\nu y\right)$	$-\frac{4\sqrt{3}}{15}(1+2g_\nu y)$		$\frac{2\sqrt{10}}{15}(1+2g_\nu y)]$		
	0	$\frac{4}{15\sqrt{3}}\left(1-\frac{1}{2}g_s y\right)$	$-\frac{4}{15\sqrt{2}}(1+2g_s y)$		$\frac{2\sqrt{5}}{15\sqrt{3}}(1+2g_s y)$		
$M4$	1	$\frac{2\sqrt{14}}{7}g_\nu$					
	0	$\frac{2\sqrt{7}}{7\sqrt{3}}g_s$					

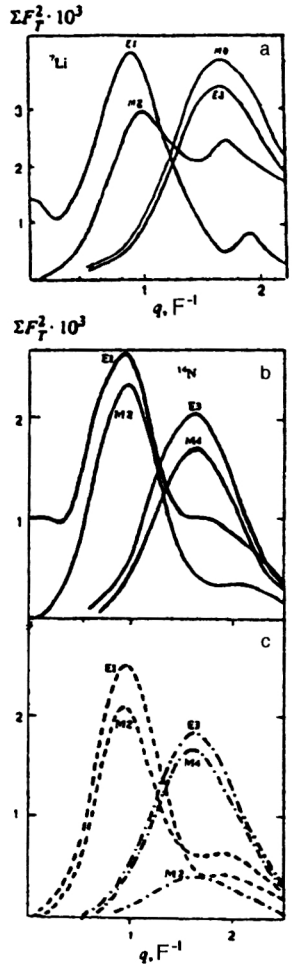

FIG. 1. Squares of the total transverse form factors of $1\hbar\omega$ excitations of the nuclei (a) ^{7}Li and (b) ^{14}N (solid lines). (c) The dashed lines are the contributions of the spin-dipole excitation modes, and the dot–dash lines are the contributions of the spin-octupole modes to multipole resonances of ^{14}N (Ref. 20).

transverse form factors of $1p$- and $1d-2s$-shell nuclei is based on study of the structure of the single-particle form factors of $1\hbar\omega$ transitions forming MRs. Since the same single-particle configurations enter into the MR wave functions of different nuclei of the same shell, on the graphs of the form factors of single-particle excitations we shall indicate the values of **F**, related to the form factors F of (2.4) as

$$\mathbf{F}=\frac{Z}{(4\pi)^{1/2}}(J_i+1)^{1/2}F. \tag{3.1}$$

The values of **F** are independent of the nuclear characteristics and for single-particle transitions are equal to the matrix elements of the multipole operators multiplied by the corrections f_{SN} (2.18) and $f_{\rm cm}$ (2.19).

3.1. Single-particle $E1$ transitions in light nuclei

The behavior of the form factors of single-particle $E1$ transitions from the $1p$ shell and the contributions to them from the orbital and spin components are shown in Fig. 3. In Fig. 4 we give the squares of these form factors on a logarithmic scale together with the longitudinal $C1$ form factors. Measurement of the longitudinal and transverse form factors of the same multipole excitation EJ not only allows the separation of electric and magnetic MRs close in energy, but in some cases can help to identify the single-particle transition dominating in MR formation. Comparison of the q dependences of the $E1$ form factors for $1p_{3/2}\rightarrow 1d_{5/2}$ and $1p_{3/2}\rightarrow 1d_{3/2}$ transitions is an example of such a possibility. In the first transition the contributions to the form factor from orbital currents generated by the operators $[Y_0\times\hat{\nabla}]_1$ and $[Y_2\times\hat{\nabla}]_1$ (henceforth denoted as the $B0$ and $B2$ components) are important at small momentum transfers, where they form the principal maximum of the photonuclear giant dipole resonance (GDR). For $q<0.3$ F^{-1} the contributions of orbital currents dominate over those of spin currents for all transitions. For the second transition the contribution of the orbital current is negligible even at low q, and the transition form factor is formed practically only by the spin component of the current. Of the other $E1$ transitions from the $1p$ shell, the matrix elements of the operators for the orbital currents of the $1p_{1/2}\rightarrow 1d_{3/2}$ transition are the largest. A result of this distribution of the matrix elements of the orbital currents of the $E1$ excitation is the well known dominance of the contributions of $1p_{3/2}\rightarrow 1d_{5/2}$ transitions to the GDR wave functions. The $1p_{1/2}\rightarrow 1d_{3/2}$ transitions give the second largest contribution to the cross section for the photonuclear giant resonance.[12,15]

Increase of the momentum transfer leads to increase of the absolute value of the matrix element of the spin current generated by the spin–angular operator $[Y_1\times\hat{\sigma}]_1$ (henceforth denoted as $A1$). For some single-particle processes the interference between the orbital and spin components is destructive and leads to the appearance of zeros in the corresponding form factors. These are manifested as minima in the squared form factors (Fig. 4) of nondiffraction origin. An example of such a feature is the minimum of F^2 for the $1p_{3/2}\rightarrow 1d_{5/2}$ transition at $q\approx 0.5$ F^{-1}, which is the result of the interference of the orbital and spin components and the passage of the corresponding form factor through zero. A similar situation arises in the behavior of the form factor of the $1p_{1/2}\rightarrow 2s_{1/2}$ transition, where the interference of the contributions of the two currents also leads to the appearance of a nondiffraction zero.

As the momentum transfer grows, the relative importance of the spin currents in the form factors grows. Above $q=1.0$ F^{-1} the effect of the nucleon orbital current on the behavior of the form factors is manifested only in shifts of the diffraction minima in Fig. 4. It should be emphasized that the minima of the longitudinal CJ form factors (Fig. 4) coincide with the minima of the spin-current contributions to the form factor of the EJ transition, and in both cases are consequences of the passage of the matrix elements of the spherical Bessel function $j_J(qr)$ through zero. All five single-particle $E1$ transitions from the $1p$ shell are characterized by the presence of a diffraction minimum at $q>1$ F^{-1}, the exact location of which in each case depends on the specific form of the polynomial $P_{EJ}(y)$. Analysis of the behavior of the form factors of single-particle $C1$ and $E1$ transitions (Fig. 4) shows that the ratio of the longitudinal and transverse form factors depends both on the momentum

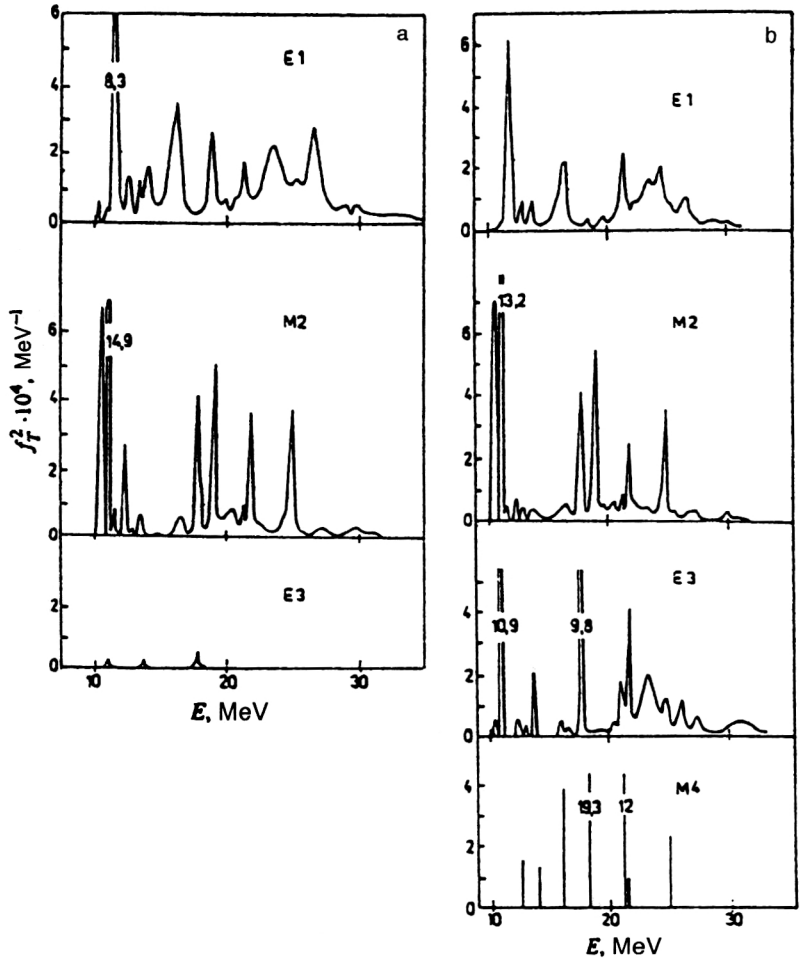

FIG. 2. Energy distribution of intensities of multipole $1\hbar\omega$ excitations of ^{15}N at the momentum transfers (a) 0.7 F^{-1} and (b) 1.3 F^{-1} (Ref. 16).

transfer q and on the specific single-particle transition. For example, for $1p_{3/2} \rightarrow 1d_{5/2}$ and $1p_{1/2} \rightarrow 1s_{1/2}$ transitions in the region $q \approx 1.2$ F^{-1}, the destructive interference of the spin and convection modes causes the form factors of these $E1$ transitions to have their first minimum approximately at the maximum of the single-particle $C1$ form factor. Another consequence of the destructive interference is that the absolute values of the form factors of these two $E1$ transitions near the maxima turn out to be considerably smaller than the values of the corresponding longitudinal $C1$ form factors, while in the other cases the first maxima of the single-particle $C1$ and $E1$ form factors are comparable in magnitude. The ratio F_{C1}^2/F_{E1}^2 for individual resonances is sensitive to the details of the configurational structure of the dipole excitations. Comparison of the q dependences of the longitudinal and transverse form factors at momentum transfers below 1 F^{-1} can therefore help in identifying the quantum numbers of the transition dominating in the MR wave function. In $1d-2s$-shell nuclei the transverse form factors of $E1$ transitions have a somewhat more complicated structure than for lighter nuclei. This is a consequence of the higher powers in the polynomials $P_J(y)$ in (2.28)–(2.30). In Fig. 5 we show the q dependences of the squared form factors for all $1\hbar\omega$ single-particle transitions from the $1d-2s$ shell. As for $1p$-shell nuclei, the interference of the orbital and spin components of the current leads to the appearance of nondiffraction minima in the form factors of several single-particle transitions. These minima occur for momentum transfers $q < 1$ F^{-1}, when the contribution of the orbital components to the transverse form factor of several transitions is fairly large, and the orbital and spin components have opposite signs. The $1d_{5/2} \rightarrow 1f_{7/2}$, $2s_{1/2} \rightarrow 2p_{3/2}$, and $1d_{3/2} \rightarrow 2p_{3/2}$ transitions are such transitions, and in them the destructive interference of the orbital and spin components leads to a sharp contrast in the behavior of the longitudinal and transverse form factors of a given excitation.

3.2. $E1$ resonances in the electroexcitation cross sections of light nuclei

As is well known, the excitation of electric dipole ($E1$) resonances in photonuclear reactions is associated with the operator $\hat{\tau}_3 r Y_1(\Omega)$, and, therefore, practically only the spinless part of the intranuclear nucleon current is manifested in such reactions. The situation is similar in (e,e') reactions at small momentum transfers ($q < 0.3$ F^{-1}): $E1$ excitations are mainly produced by the spinless operators $\hat{\tau}_3 j_0(qr)[Y_0 \times \hat{\nabla}]_1$ and $\hat{\tau}_3 j_2(qr)[Y_2 \times \hat{\nabla}]_1$ [see (2.14)], reflecting the contribution of the convection current of the charge motion. However, as q increases further the contribution of the spin component of the nucleon current associated with the spin-dipole operator $\hat{\tau}_3 j_1(qr)[Y_1 \times \hat{\sigma}]_1$ becomes more important.

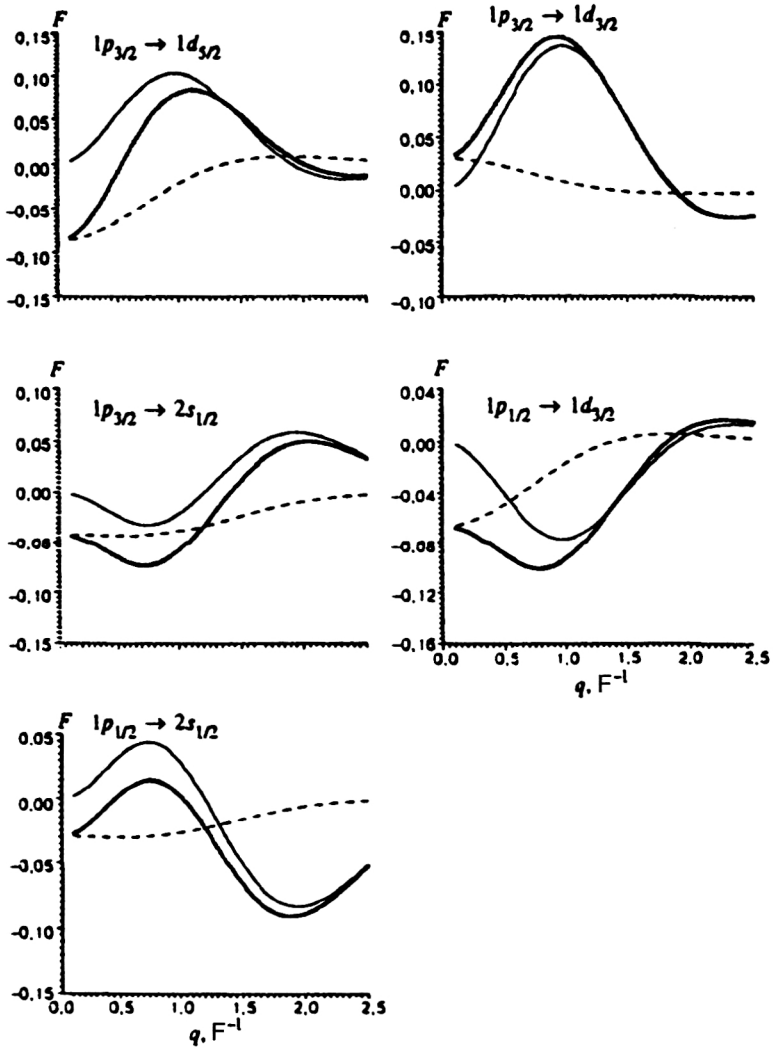

FIG. 3. Form factors of single-particle $E1$ transitions in $1p$-shell nuclei. The thin solid lines are the contributions of the spin current to the form factor, the dashed lines are the contributions of the orbital current, and the heavy solid lines are the $E1$ form factors (calculation with oscillator parameter equal to 1.67 F^{-1}).

Therefore, in contrast to photonuclear reactions, in electroexcitation it is possible to study the spin mode of the $E1$ resonance.

For (e,e') dipole electroexcitation reactions it is possible to study the spin and spinless components of the electric dipole modes separately, since the transverse $E1$ form factors receive contributions from both the spin and the convection components, while the longitudinal $C1$ form factors arise almost entirely from spinless modes.

The microscopic analysis of $E1$ resonances in electroexcitation reactions performed in Refs. 22–25 showed that the spin components of $E1$ excitations are manifested most clearly in the form of a maximum of the transverse form factor located roughly at $q=0.8-1.2$ F^{-1} and, as a rule, localized at a somewhat higher energy than the principal maximum of the "photonuclear" dipole resonance. These $E1$ excitations are referred to as the spin–isospin or transverse dipole resonance.

It is natural to begin analyzing the relative contributions of the spin and convection modes of dipole excitations with the ^{12}C nucleus, which in the PCC model has the simplest ground-state configuration. In the calculations of the excited states of this nucleus the PCC basis was extended by including $(J'T'E')$ configurations genetically related not only to the ground state, but also to the first excited state. The results of the PCC calculation of $E1$ excitations for ^{12}C (Ref. 25) are shown in Fig. 6, where we give the energy distribution of the transverse form factors of $E1$ transitions at three values of the momentum transfer q. At $q=0.2$ F^{-1} the picture of dipole excitations is very close to the distribution of cross sections for the photonuclear reaction,[10,12,26] which corresponds to the "photopoint" of the transverse form factor $(q=\omega)$. At small momentum transfers the cross section for inelastic electron scattering is dominated by the peak of the 1^-, $T_f=1$, $E=22.8$ MeV giant dipole resonance, whose wave function is mainly determined by the $|(3/2)_1(1d_{5/2})\rangle$ configuration.[10] This configurational structure of the excited state must, according to Fig. 3, lead to a minimum in the form factor for $q\approx 0.5$ F^{-1}. The 1^- states, whose wave functions contain large components from configurations corresponding to the $1p_{3/2}\rightarrow 1d_{5/2}$ transition, must contribute significantly to the cross section not only in the vicinity of the photopoint, but also at momentum transfers $q \approx 0.7-1.5$ F^{-1} (see Fig. 6), where $E1$ resonances are excited by contributions from the spin-dipole operator. Meanwhile, at $q>0.3$ F^{-1} not only do the contributions of the spin-dipole modes as a whole begin to grow (Fig. 5), but also the $E1$ excitations due to the $1p_{3/2}\rightarrow 1d_{3/2}$ spin-flip transition

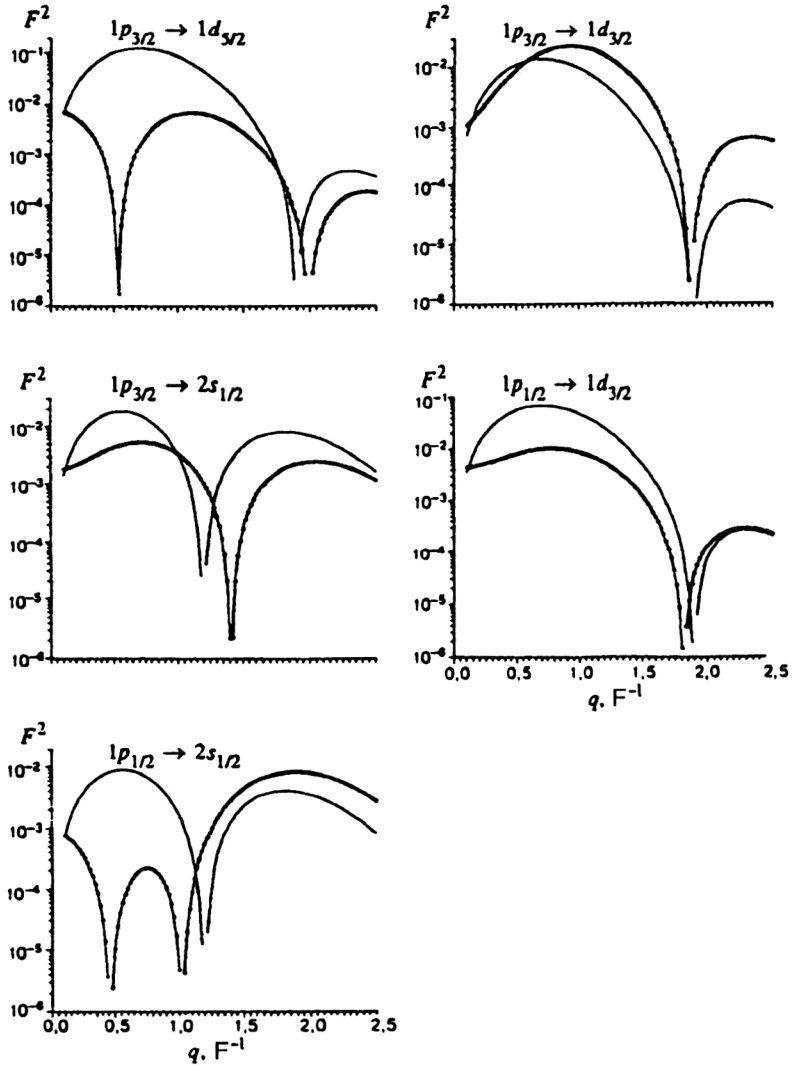

FIG. 4. Squares of the transverse $E1$ form factors (heavy lines) and longitudinal $C1$ form factors (thin lines) of single-particle transitions in $1p$-shell nuclei.

become more important in the cross section. As a result, the weighted mean energy of dipole transitions is shifted upward in excitation energy (Table II), and already at $q=0.5$ F^{-1} the principal maximum of the energy distribution of the transverse $E1$ form factors of ^{12}C turn out to be localized at $E=24.9$ MeV. This state corresponds to the spin–isospin dipole resonance in the ^{12}C nucleus. Its wave function is the result of the mixing of many configurations, but those with largest amplitude are the $|(3/2)_1(1d_{3/2})\rangle$ and $|(1/2)_1(1d_{3/2})\rangle$ configurations,[25] the first of which corresponds to the $1p_{3/2} \rightarrow 1d_{3/2}$ spin-flip transition. At the peak of the dipole excitation of ^{12}C at $E=22.8$ MeV, the longitudinal form factor in the range 0.2 F$^{-1}<q<1.5$ F^{-1} is roughly an order of magnitude larger than the transverse form factor, owing to the dominant contribution to the wave function from the single-particle $1p_{3/2} \rightarrow 1d_{5/2}$ transition. Experimental data obtained more than 20 years ago[31] show that the longitudinal form factor is considerably larger than the transverse one for the maximum of the cross section at $E=22.7$ MeV.

According to the calculations, the longitudinal form factor of the 1^-, $E=24.9$ MeV state is also slightly larger than the transverse form factor, despite the large contribution of the $1p_{3/2} \rightarrow 1d_{3/2}$ spin-flip transition. This excess is associated with contributions to the excitation from the $1p_{1/2} \rightarrow 1d_{3/2}$ transition, since for it $F^2_{C1}>F^2_{E1}$, in contrast to the $1p_{3/2} \rightarrow 1d_{3/2}$ transition. Nevertheless, the significant role played by the spin-flip component in forming this resonance is seen from the fact that for it $(F^2_{C1}/F^2_{E1})_{24.9} < (F^2_{C1}/F^2_{E1})_{22.8}$. Given this strongly contrasting behavior of the $C1$ and $E1$ form factors in these two cases, it would be very desirable to perform a more detailed experimental study of the dipole excitations of the ^{12}C nucleus in (e,e') reactions with the contributions of the two form factors distinguished.

For nuclei with $T_i \neq 0$ the microscopic analysis of dipole excitations is somewhat complicated by the existence of two isospin branches: $T_<$ and $T_>$. Therefore, an interesting object for studying dipole resonances is the ^{14}C nucleus, which has, on the one hand, zero spin in the ground state and, on the other, nonzero isospin ($T_i=1$), leading to the presence of two branches of multipole excitations: $T_f=1$ and $T_f=2$. The theoretical analysis of photodisintegration of the ^{14}C nucleus performed using the PCC model in Ref. 14 gave reasonable agreement with the data from photoneutron and photoproton experiments[27–29] for this nucleus. The distribu-

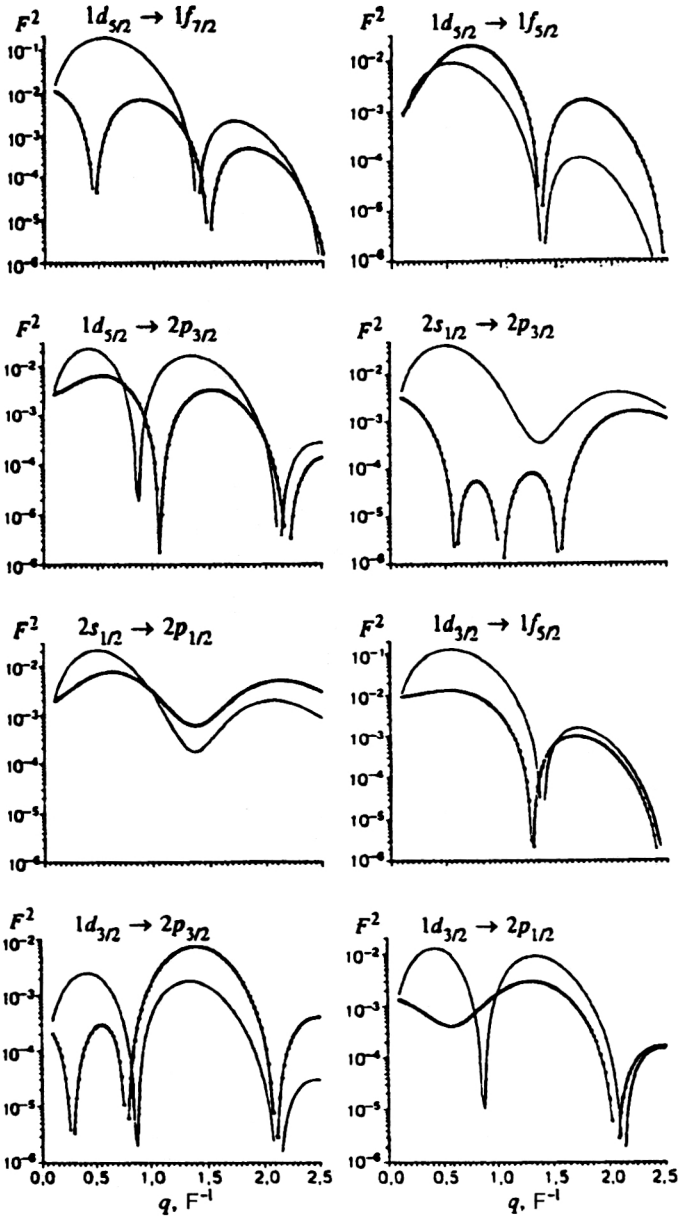

FIG. 5. Squares of the single-particle form factors of dipole excitations of $1d-2s$-shell nuclei. The notation is the same as in Fig. 4 (calculation with oscillator parameter equal to 1.85 F^{-1}).

tion of intensities of $E1$ form factors of the ^{14}C nucleus obtained in Ref. 24 at momentum transfers above the photopeak is given in Fig. 7. As in the case of electrodisintegration of the ^{12}C nucleus, for $q<0.2$ F^{-1} the convection-current contributions dominate and the distribution of transverse form factors is very close to that for the photonuclear dipole resonance, while for $q>0.2$ F^{-1} states whose excitation receives a large contribution from the spin current begin to dominate. In particular, the 1^-, $T_f=1$, $E=23.4$ MeV and 1^-, $T_f=2$, $E=30.6$ MeV peaks, which determine the electroexcitation cross section at $q\approx 0.5$ F^{-1} (Fig. 7b), are formed mainly by configurations associated with the $1p_{3/2} \to 1d_{3/2}$ transition.

We see from Table II that the weighted mean energy of $E1$ excitations grows with increasing q for both isospin branches. However, the $T_f=2$ states are localized at higher excitation energies than the $T_f=1$ states. For momentum transfers close to the photopoint (Fig. 7a), the $T_<$ branch plays the main role in the formation of so-called pygmy resonances: relatively broad peaks at low energies, while the principal maximum of the dipole resonance is associated with excitation of the $T_>$ branch. As q increases further the principal maxima of the $T_<$ branch of the spin–isospin $E1$ resonance begin to be clearly manifested. They are separated from the principal $T_>$ peaks by an energy interval of about 6–7 MeV (Figs. 7b and 7c). However, it should be noted that at high energies ($E>25$ MeV), where the dominant contribution to the $E1$ excitation cross section comes from the $T_>$ branch, states with $T_<$ also play an important role, as can be seen from Fig. 7. This is associated with the stronger fragmentation in excitation energy of the $T_<$ branch relative to the $T_>$ branch.

The fragmentation strength of multipole excitations in even–even $1p$-shell nuclei is primarily a consequence of the distribution of $(1p_{3/2}^{-1})$ and $(1p_{1/2}^{-1})$ hole configurations among the core states. For the ^{14}C nucleus the separation of

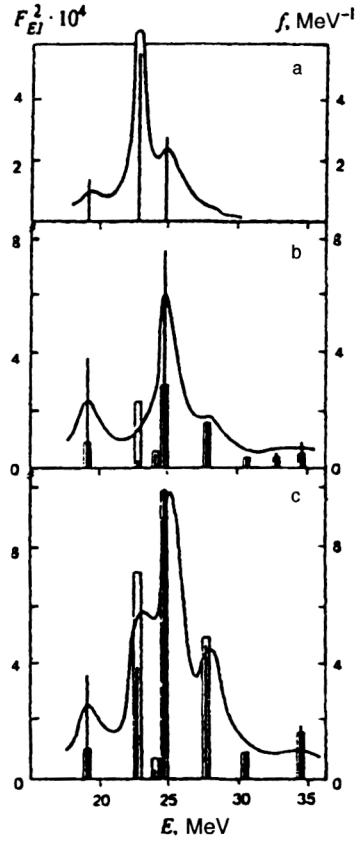

FIG. 6. Energy distribution of form factors of $E1$ excitations of the ^{12}C nucleus at momentum transfers (a) 0.2 F^{-1}, (b) 0.5 F^{-1}, and (c) 1.0 F^{-1} (Ref. 24). The solid lines are the form factors neglecting the widths, and the bars are the contributions of the spin current. The curves are the $E1$ form factors including the decay widths (right-hand scale).

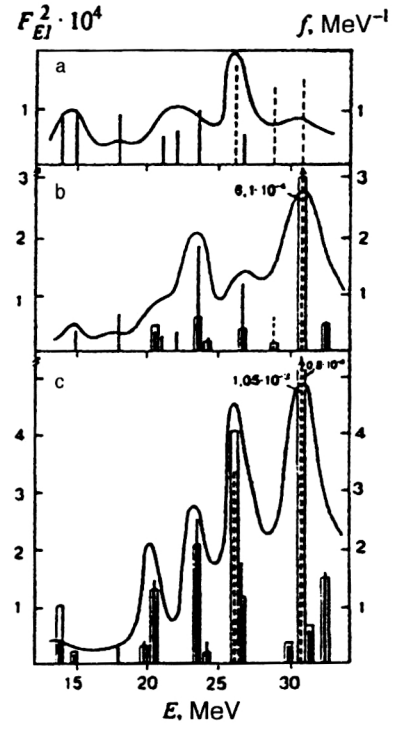

FIG. 7. Energy distribution of the form factors of $E1$ excitations of the ^{14}C nucleus at momentum transfers (a) 0.2 F^{-1}, (b) 0.5 F^{-1}, and (c) 1.0 F^{-1} (Ref. 24). The solid straight lines are the form factors of states with isospin 1, and the dashed straight lines are the form factors of states with isospin 2. The rest of the notation is the same as in Fig. 6.

a $1p$ nucleon from the ground state leads to a broad spectrum of levels of nuclei with $A=13$. For excited 1^-, $T_f=1$ states the wave functions are mainly formed by the nine states of the ^{13}C and ^{13}B nuclei with sizable genetic coupling to the ^{12}C ground state. The experimental study of the real fragmentation of excited nuclear states tests not only the reliability of the theoretical approach on the whole, but also the structure of the ground-state nuclear wave function used in the calculations.

The configurational structure of the $T_f=2$ branch of dipole excitations of the ^{14}C nucleus is considerably simpler than that of the $T_f=1$ branch, because only $T'=3/2$ states of $A=13$ nuclei are involved in its formation. Near the maximum of the spin–isospin dipole resonance, where $q \approx 1$ F^{-1}, the two peaks at 26.4 MeV and 30.6 MeV dominate in the $T_f=2$ branch. The first of these is mainly excited in the $1p_{3/2} \rightarrow 1d_{5/2}$ transition, and it is also the principal maximum of the photonuclear dipole resonance. The second, as noted above, corresponds almost completely to the $1p_{3/2} \rightarrow 1d_{3/2}$ spin-flip transition. The behavior of the $C1$ and $E1$ form factors of these states is shown in Figs. 8a and 8b.

In contrast to high-lying $T_f=2$ states, the 1^-, $T_f=1$, $E=13.7$ MeV and 1^-, $T_f=1$, $E=14.7$ MeV dipole-excitation peaks, which probably correspond to the experimentally observed 1^-, $T_f=1$, $E=13.62$ MeV level,[30] are strongly collectivized. The $E1$ form factors of these two states pass through their second maximum at $q \approx 1.7$–1.8 F^{-1}, when the electroexcitation cross section is mainly formed by resonances of higher multipole order. According to the results of (e,e') experiments at scattering angle 180° performed at the MIT Bates accelerator,[30] a peak at excitation energy 13.5–14 MeV is actually observed at large momentum transfers, although its intensity is quite weak compared to the $M4$ resonances dominating in this region. The experimental data for the q dependence of the form factor of the 13.62 MeV state given in that study also indicate the presence of a maximum at $q \approx 1.8$ F^{-1}, which corresponds to the theoretical predictions.

As in the case of ^{12}C, the experimental study of the quantitative ratios of the longitudinal and transverse form factors of the principal maxima of the cross sections for dipole electroexcitation of ^{14}C can serve as the basis for a microscopic analysis of the configurational structure of the MR wave functions.

TABLE II. Mean energies of $E1$ resonances in $1p$-shell nuclei.

		$\bar{E}=(\Sigma F_i^2 E_i)/F_i^2$ (MeV)		
Nucleus	T_f	$q=0.2$ F^{-1}	$q=0.5$ F^{-1}	$q=1.0$ F^{-1}
^{12}C	1	23.4	24.6	25.4
^{14}C	1	17.9	18.8	20.0
	2	28.4	30.4	29.6

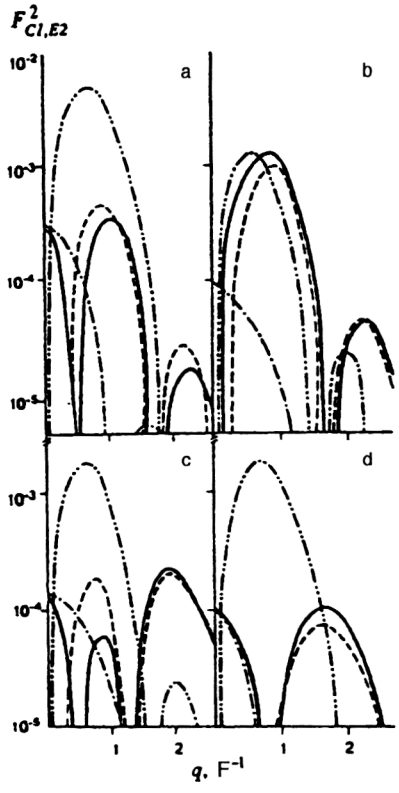

FIG. 8. $C1$ and $E1$ form factors of four 1^- states of the ^{14}C nucleus. (a) Level with $E=26.4$ MeV, $T=2$; (b) $E=30.6$ MeV, $T=2$; (c) $E=13.7$ MeV, $T=1$; (d) $E=14.7$ MeV, $T=1$. The solid lines are the $E1$ form factors, the dashed lines are the contributions to them from spin-dipole modes, the dot–dash lines are the contributions to them from orbital modes, and the dashed lines with two dots are the longitudinal form factors $C1$ (Ref. 24).

4. MAGNETIC QUADRUPOLE EXCITATIONS OF LIGHT NUCLEI

Both spin and convection modes participate in forming $M2$ resonances of light nuclei. In contrast to $E1$ excitations, the contributions of orbital currents to $M2$ transitions are very insignificant in the entire range of momentum transfers ($B2$ in Figs. 9 and 10).

The distinctive feature of magnetic quadrupole excitations in nuclei is the fact that the contributions of the spin current to their formation arise from two types of spin operator: the spin-dipole operator $[Y_1\times\hat{\sigma}]_2$ and the spin-octupole operator $[Y_3\times\hat{\sigma}]_2$. The corresponding contributions to the form factors are denoted as $A1$ and $A3$ on the graphs.

4.1. Single-particle form factors of $M2$ excitations

The distributions of the squared single-particle form factors of transitions from the $1p$ shell are shown in Fig. 9.

In $1p$-shell nuclei $M2$ excitations are realized by five single-particle transitions: $1p_{3/2}\to 1d_{5/2}$, $1p_{3/2}\to 1d_{3/2}$, $1p_{3/2}\to 2s_{1/2}$, $1p_{1/2}\to 1d_{5/2}$, and $1p_{1/2}\to 1d_{3/2}$. The convection-current contribution is absent in the case of the $1p_{3/2}\to 2s_{1/2}$ transition. Moreover, the spin mode of this transition is formed only by the operator $[Y_1\times\hat{\sigma}]_2$. Therefore, the $M2$ form factor due to the $1p_{3/2}\to 2s_{1/2}$ transition is a purely spin-dipole form factor. Accordingly, its q dependence is the same as that of the spin component of the corresponding $E1$ resonance. Convection currents are present in the other $M2$ transitions, but their effect is insignificant. The orbital-current contribution is most important in the $1p_{1/2}\to 1d_{3/2}$ transition, where the interference of the orbital and spin components, which at small q are comparable in magnitude and have opposite signs, leads practically to the absence of a significant contribution from the $M2$ form factor to the electroexcitation cross section at $q<0.6$ F^{-1}. The maximum of the form factor of this transition at momentum transfers of about 1.7 F^{-1} corresponds to the maximum of the spin-octopole contribution $A3$. The spin-octupole operator dominates in $M2$ transitions to the $1d_{3/2}$ subshell at momentum transfers above 1.2 F^{-1}.

The behavior of the form factors of $M2$ excitations at small momentum transfers is primarily determined by the contributions of the first maxima of the form factors of single-particle $1p_{3/2}\to 1d_{5/2}$ and $1p_{1/2}\to 1d_{5/2}$ transitions, which are formed almost entirely by the spin-dipole mode.

In Fig. 10 we show the q dependences of the squared form factors of all single-particle $M2$ transitions from the $1d-2s$ shell, and also the contributions of the orbital ($B2$) and spin ($A1$ and $A3$) components of the nucleon current. Obviously, for these nuclei, as for $1p$-shell nuclei, orbital currents play a small role in $M2$ excitations. The orbital current is manifested most significantly in the $1d_{3/2}\to 1f_{5/2}$ transition, where its destructive interference with the spin current leads to very small values of the $M2$ form factor up to momentum transfers $q>0.8$ F^{-1}. The very small values of the $M2$ form factors for the $1d_{3/2}\to 2p_{1/2}$ transition at low q have a similar origin. For the other form factors of $M2$ transitions the orbital current is manifested as a small shift in the location of the diffraction minimum. The form factors of transitions from the $2s$ subshell do not contain any orbital-current contributions.

The effect of the values of the g factors on the magnitude and behavior of the form factors was traced for all $M2$ single-particle transitions. The distribution of multipole form factors at $g=0.7g_{\text{bare}}$ remains close to the distribution at $g=1.0g_{\text{bare}}$, although the squared form factors at the maxima are lower by a factor of two. As the g factors decrease the contributions of the orbital currents remain about the same, which ultimately leads to small shifts in the locations of the minima of the squared form factors. These changes are very minor and do not offer any possibility of determining the nucleon g factors in nuclear excitations from analysis of the features of the transverse form factors.

4.2. $M2$ resonances in the electroexcitation of light nuclei

Spin-dipole and spin-octupole $M2$ excitation modes in the electroexcitation of $1p$-shell nuclei produce effects which are sensitive to the individual properties of specific nuclei. However, the behavior of the $M2$ form factors displays some general trends which can be traced for the example of even nuclei.

In Fig. 11 we show the energy distributions of the $M2$

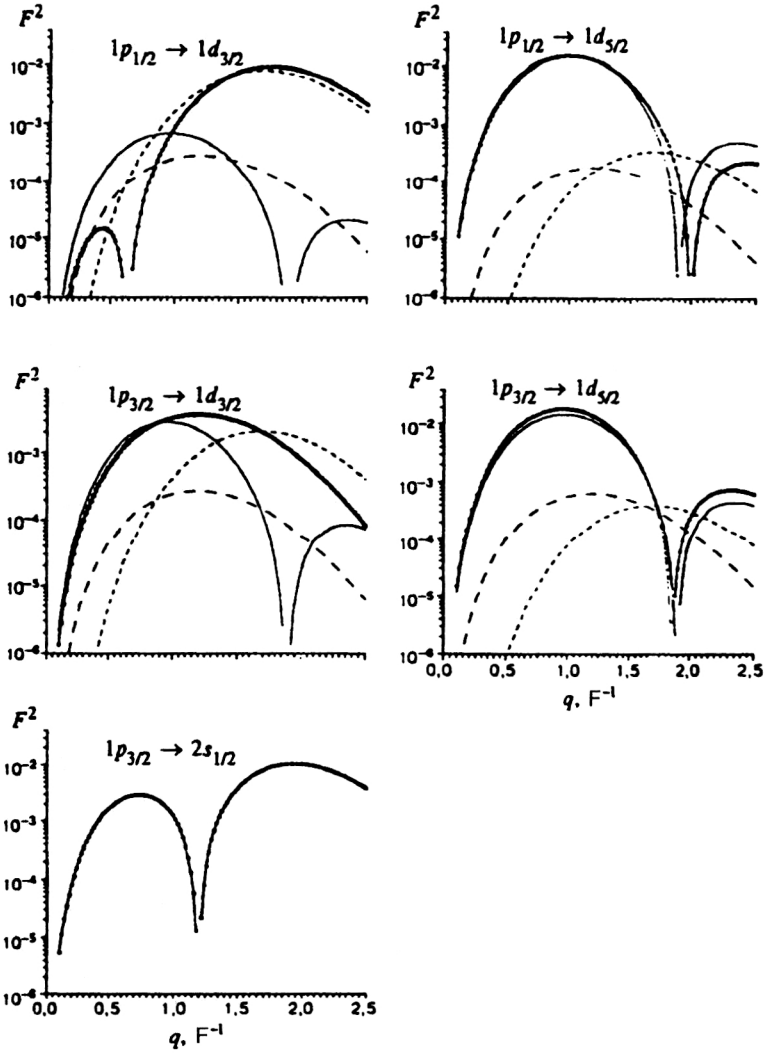

FIG. 9. Squared form factors of single-particle $M2$ transitions in $1p$-shell nuclei (calculation using the parameter $b = 1.67$ F^{-1}). The solid curves are for $A1$, the short–dash curves are for $A3$, the long–dash curves are for $B2$, and the points are for $M2$.

form factors of the ^{12}C nucleus obtained using the PCC model[33,34] for $q=0.5$, 1.0, and 1.7 F^{-1}. It should be noted that for heavier nuclei it is characteristic for the mean energy of magnetic quadrupole excitations to be shifted downward relative to the mean energy of the $E1$ resonance (see, for example, Ref. 35), while in the case of light nuclei this effect is not so strong, owing to the less significant role of collective effects in these nuclei.

The separate contributions of the spin-octupole components are shown in Fig. 11. Analysis of the contributions of the spin-dipole and spin-octupole current operators to $M2$ excitations of light nuclei has shown that the spin-octupole modes begin to be important in $M2$ excitations at momentum transfers $q>1.0$ F^{-1}. The contributions of the spin-octupole operator to $M2$ resonances reach a maximum at $q \approx 1.7$ F^{-1}. They play a large role in magnetic quadrupole excitations if the wave function of a given state contains a significant fraction of configurations corresponding to single-particle $1p_{1/2} \to 1d_{3/2}$ and $1p_{3/2} \to 1d_{3/2}$ transitions. Single-particle $1p_{3/2} \to 2s_{1/2}$ transitions must dominate in the wave functions of states having intense maxima of spin-dipole nature in roughly the same range of momentum transfers ($q \approx 1.8$–1.9 F^{-1}). Therefore, the picture of the electroexcitation of $M2$ resonances at 1.5 F$^{-1} < q < 2$ F^{-1} is mainly determined by the contributions of three single-particle transitions: $1p_{1/2} \to 1d_{3/2}$, $1p_{3/2} \to 1d_{3/2}$, and $1p_{3/2} \to 2s_{1/2}$.

The increase of the mean energy of $M2$ resonances with increasing momentum transfer to the nucleus is reflected in Table III (Refs. 16 and 34). The growth of the weighted mean $M2$ excitation energy is related to the growth of the relative contributions of the spin-octupole $1p_{1/2} \to 1d_{3/2}$ and $1p_{3/2} \to 1d_{3/2}$ transitions. Another reason which partially explains the upward shift of the mean energies of $M2$ resonances is the higher degree of energy localization of $1p_{3/2} \to 2s_{1/2}$ transitions.

The growth of the weighted mean $M2$ excitation energy as the contribution of the spin-octupole component increases is manifested more clearly for intermediate nuclei,[36] where collective effects play the main role in exciting multipole resonances. In nuclei where the degree of collectivization is low, the features of the genetic structure make the picture of the distribution of spin-dipole and spin-octupole $M2$ resonance modes rather ambiguous. For example, the lowest 2^-, $T_f=1$ level of the ^{12}C nucleus ($E=16.58$ MeV), the q dependence of which is shown in Fig. 12a together with the data from (e,e') experiments performed in Mainz[37] and the Bates Laboratory at MIT,[38] is formed mainly by the spin-octupole components in the PCC model.[34] This is a conse-

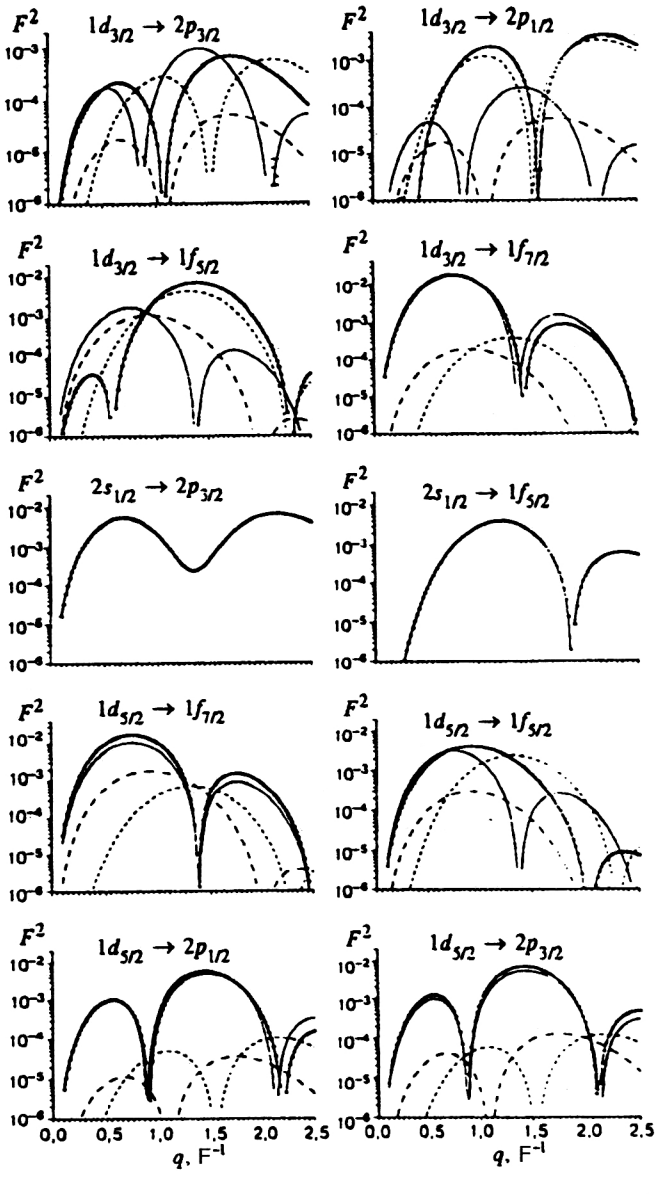

FIG. 10. Squared form factors of single-particle $M2$ transitions in $1d-2s$-shell nuclei (calculation using the parameter $b=1.85$ F^{-1}). The notation is the same as in Fig. 9.

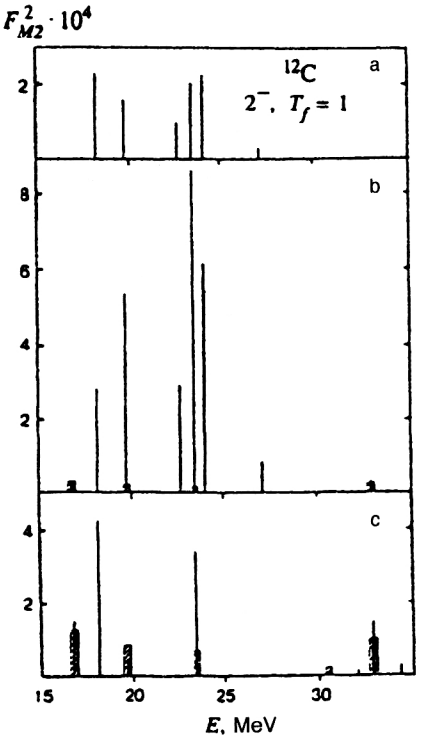

FIG. 11. Energy distribution of the form factors of $M2$ excitations of ^{12}C at momentum transfers (a) 0.5 F^{-1}, (b) 1.0 F^{-1}, and (c) 1.7 F^{-1} (Ref. 34). The shaded bars are the contributions of the spin-octupole modes.

quence of the large values of the amplitudes of the $|(1/2)_1(1d_{3/2})\rangle$ and $|(3/2)_1(1d_{3/2})\rangle$ configurations in the wave function of the lowest 2^- level of ^{12}C. According to the calculations of Refs. 38 and 39, the $|(3/2)_1(2s_{1/2})\rangle$ configuration is the most important in exciting this level of ^{12}C.

Comparison of the experimental behavior of the form factor of the 2^-, $T_f=1$, $E=16.58$ MeV state with the q dependences of the single-particle $M2$ form factors shows that the $1p_{3/2}\to 2s_{1/2}$ transition cannot give the decisive contribution to the excitation of that state, because this would require the form factor to have two maxima of comparable magnitude at $q\approx 0.7$ F^{-1} and 2 F^{-1}, which is not consistent with the experimental picture. The data of Ref. 37 indicate the presence of a very weak first maximum in the form factor of the state with $E=16.58$ MeV at small q (Fig. 9a). This implies that a realistic wave function of this state must contain, in addition to the $|(1/2)_1(1d_{3/2})\rangle$ and $|(3/2)_1(1d_{3/2})\rangle$ configurations, also the $|(3/2)_1(2s_{1/2})\rangle$ configuration with small amplitude, responsible for forming the first maximum. The suggestion in Ref. 37 that the interference of the spin and orbital currents can lead to the suppression of the first maximum appears unlikely, owing to the insignificant role played by orbital currents in the excitation of $M2$ transitions (and in the HOWF approximation this contribution is equal to zero for the $1p_{3/2}\to 2s_{1/2}$ transition). Therefore, one of the possible ways of solving the problem of the structure of the wave functions of excited states of light nuclei is by analyzing the features of the experimental form factor and comparing it with the single-particle form factors.

A configurational structure of this type is predicted by the PCC calculations also for the low-lying 2^-, $T_f=1$, $E=14.72$ MeV level in ^{14}N, which is the result of the coupling of two valence nucleons to the 2^-, $T_f=1$, $E=16.58$ MeV state of ^{12}C. The experimental behavior of the form factor of the level at $E=14.72$ MeV (Ref. 40) is reproduced well by the PCC calculations[33] (Fig. 13a).

According to the results of Refs. 33 and 42, in the ^{14}C nucleus there must also be a low-lying 2^-, $T_f=1$ level of spin-octupole nature. In Fig. 13b we compare the q dependence of the form factor of this state with the experimental data[41] for the 15.96 MeV level of ^{14}C. Although in Ref. 41 the quantum numbers for the peak at 15.96 MeV were not determined, the behavior of its form factor corresponds to the theoretical q dependence of the form factor of the 2^-, $T_f=1$ state of lowest energy in the calculation of Ref. 33.

Thus, the PCC calculations predict the presence of low-lying 2^-, $T_f=1$ states for all three nuclei, with the $|(1/2)_1(1d_{3/2})\rangle$ and $|(3/2)_1(1d_{3/2})\rangle$ configurations playing an

TABLE III. Shifts of mean energies of $M2$ resonances in $1p$-shell nuclei.

Nucleus	^{12}C	^{14}C	^{14}C	^{14}N	^{15}N	^{15}N
Isospin T	1	1	2	1	1/2	3/2
$\Delta E(\text{MeV}) = \bar{E}(q=1.7\,\text{F}^{-1}) - \bar{E}(q=0.5\,\text{F}^{-1})$	0.6	3.5	6.1	1.7	2.4	3.1

important role in the wave functions of these states. Spin-octupole modes of the spin current dominate in the form factors of the corresponding $M2$ transitions. The presence of the spin-octupole mode explains the maximum in the form factors of these states at momentum transfers of about $1.7\,\text{F}^{-1}$.

In Fig. 12b we show the q dependences of the form factors of the 2^-, $T_f=1$, $E=19.35$ MeV and 4^-, $T_f=1$, $E=19.59$ MeV levels of the ^{12}C nucleus calculated in the PCC model[17] together with the experimental data[38] for the complex at 19.5 MeV. The $|(3/2)_1(1d_{5/2})\rangle$ configuration corresponding to the $M2$ transition $1p_{3/2}\rightarrow 1d_{5/2}$, dominated by the spin-dipole mode, plays the leading role in the excitation of the 2^- level. (We note that in the case of the $M4$ excitation the matrix element of this transition is formed only by the spin-octupole operator $[Y_3\times\hat{\sigma}]_4$, and so the q dependence of the $M4$ form factor of the level at 19.59 MeV differs significantly from that of the $M2$ form factor.) The observed behavior of the form factor is therefore the result of the superposition of the $M2$ and $M4$ excitations.

Conversely, the behavior of the form factors of $M2$ transitions excited mainly owing to the spin-octupole components is close to the behavior of the $M4$ form factors. Therefore, agreement between the theoretical behavior of the form factors of excited states and the experimental data cannot serve as a unique criterion for the correctness of a model description of the configurational structure of the states. Study of the partial decay channels provides an additional method of identifying the quantum numbers and configurational structure of an excited state.[42]

In Fig. 14 we show the form factors of the level at 24.4 MeV in the ^{14}C nucleus from the data of Ref. 30 and of the level at 20.1 MeV in ^{14}N from the data of Ref. 40 together

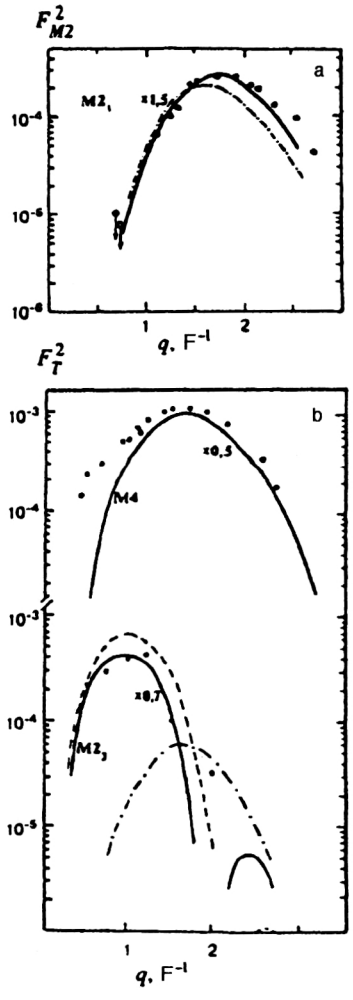

FIG. 12. Dependence of the $M2$ form factors of several levels of the ^{12}C nucleus on the momentum transfer: (a) the 2^-, $T=1$ level at $E=16.58$ MeV. The calculation is from Ref. 34, and the experimental data are from Ref. 37 (low q) and Ref. 38; (b) the complex of states of the ^{12}C nucleus at $E=19.5$ MeV. The experimental data are from Ref. 38, and the calculation of the $M2$ and $M4$ form factors is from Ref. 34.

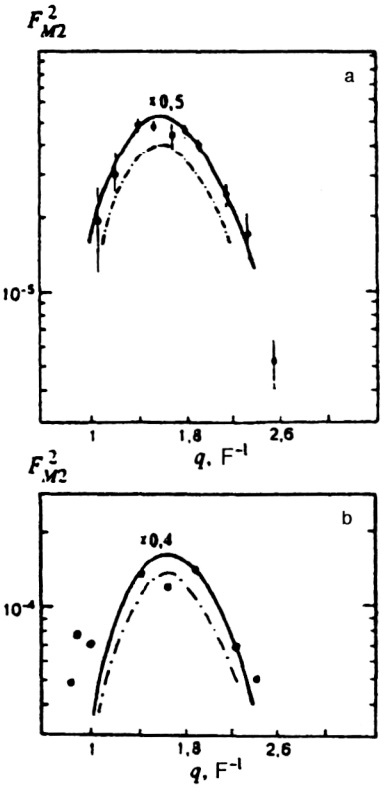

FIG. 13. Form factors of low-lying 2^-, $T=1$ states of (a) ^{14}N and (b) ^{14}C nuclei. The experimental points are from (a) Ref. 39 and (b) Ref. 41.

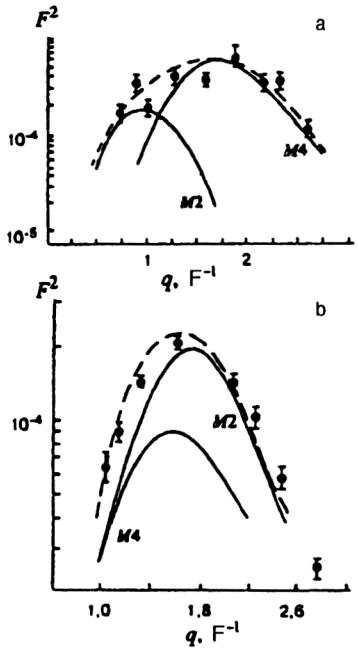

FIG. 14. $M2$ and $M4$ form factors of levels of (a) the ^{14}C nucleus at $E=24.4$ MeV and (b) the ^{14}N nucleus at $E=20.1$ MeV (Ref. 42). The experimental data are from (a) Ref. 41 and (b) Ref. 40.

with the results of the PCC calculation.[42] The theoretical calculations for ^{14}C lead to the conclusion that the behavior of the form factor of the level at 24.4 MeV is, as for the complex at 19.5 MeV in ^{12}C studied above, the result of the addition of the form factors of two states: the 2^-, $T=1$ and 4^-, $T=2$ states. The contribution of the first of these levels to the excitation of the total form factor is manifested at small momentum transfers. The form factor of this state receives important contributions from the single-particle form factors of the $1p_{3/2}\rightarrow 1d_{5/2}$ and $1p_{1/2}\rightarrow 1d_{5/2}$ transitions, which pass through a maximum at $q=1.0$ F^{-1}.

According to the calculation of Ref. 42, the level at 20.1 MeV in ^{14}N is formed by the contributions of the 4^-, $T=1$ and 3^-, $T=1$ states. Only the $M4$ form factor is involved in the electroexcitation of the first of these, while the second is excited owing to $M2$ transitions of the spin-octupole type. The data from experiments on pion scattering also suggest that both the $M4$ and $M2$ components are present in this resonance excitation.[40]

Multipole resonances of odd $1p$-shell nuclei are characterized by a very complicated structure of the cross sections, which is a consequence of the presence of two isospin excitation branches ($T_<=1/2$ and $T_>=3/2$), each of which, in turn, has several branches corresponding to different values of the total angular momentum J_f.

The energy distribution of $1\hbar\omega$ resonances of various multipole orders for the ^{15}N nucleus is shown in Fig. 2. The $M2$ excitation of this nucleus involves 62 states with $J_f=3/2$ and 5/2. As the momentum transfer to the nucleus grows, the contribution to the $M2$ excitation from the spin-octupole mode increases, and, accordingly, states of higher energy become more important. This is reflected in the shift of the mean excitation energy (Table III) and in the change of the contributions to the total excitation cross section from

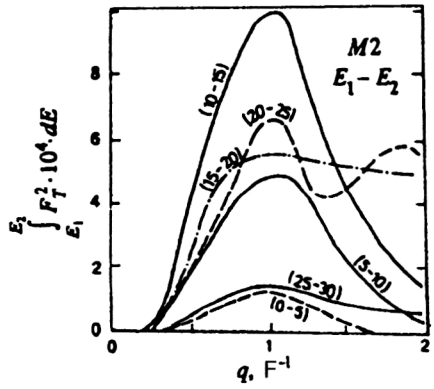

FIG. 15. Momentum-transfer dependence of the $M2$ form factors of the ^{15}N nucleus (Ref. 16).

the $M2$ form factors integrated over a given energy range (Fig. 15).

Magnetic quadrupole excitations of the ^{7}Li nucleus have the most complicated structure, as they include eight excitation branches. Their energy distribution from the results of a PCC calculation[20] is shown in Fig. 16. The large number of excitation branches leads to a quite chaotic distribution of the $M2$-transition strengths, but still we can see some of the general regularities mentioned above in the analysis of multipole excitations. In particular, we see that the fragmentation of the $T_<$ branch is stronger than that of the $T_>$ branch, and also that the $T_>$ branch has higher mean excitation energy. We also observe an increase of the weighted mean energy of $M2$ excitations with increasing q, related to the increased importance of contributions from the spin-octupole component.

5. ELECTRIC OCTUPOLE EXCITATIONS OF LIGHT NUCLEI

Study of the single-particle $E3$ form factors of light nuclei shows that it is mainly the spin-octupole mode which is involved in the excitation of the corresponding multipole resonances.

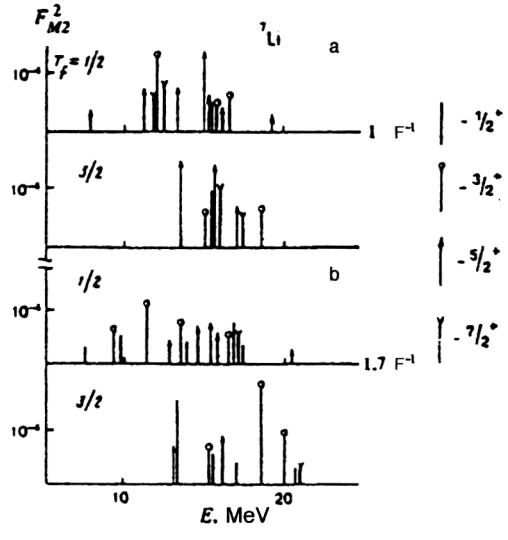

FIG. 16. Excitation-energy distribution of $M2$ form factors of the ^{7}Li nucleus at (a) $q=1.0$ F^{-1} and (b) 1.7 F^{-1} (Ref. 20).

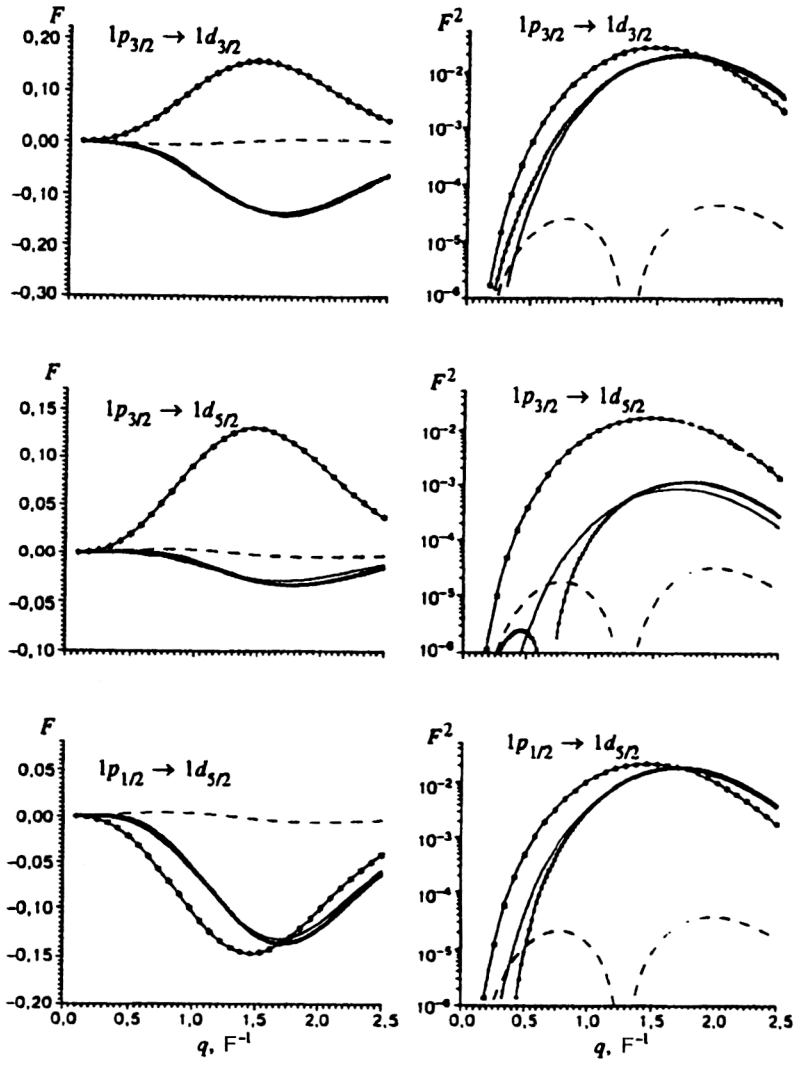

FIG. 17. Octupole single-particle excitations of $1p$-shell nuclei. On the left are the transverse $E3$ form factors (heavy solid lines) and the contributions to them from the orbital (dashed lines) and spin (heavy solid lines) components of the current. The curves with the stars are the longitudinal $C3$ form factors. On the right are the squares of these form factors on a logarithmic scale ($b=1.67$ F^{-1}).

The calculated single-particle $E3$ and $C3$ form factors for $1p$-shell nuclei are shown in Fig. 17. There we also show the contributions of the orbital and spin currents to the $E3$ form factor. The excitation of $E3$ resonances in $1p$-shell nuclei mainly occurs owing to the spin current. For the $1p_{3/2} \to 1d_{3/2}$ transition the orbital current practically does not contribute to the octupole excitation, which makes the q dependences of the transverse and longitudinal form factors similar. For the other two $E3$ transitions from the $1p$ shell, the interference of the orbital and spin currents at small momentum transfers is manifested in the appearance of a nondiffraction minimum of the $E3$ form factor. For octupole excitations of states of $1p$-shell nuclei in which the transitions $1p_{1/2} \to 1d_{5/2}$ and $1p_{3/2} \to 1d_{5/2}$ dominate, the ratios of the squared $C3$ and $E3$ form factors at small momentum transfers should be very large, owing to the interference of the orbital and spin currents.

In Fig. 18 we show the calculated form factors of octupole excitations of $1d-2s$-shell nuclei.[43] For these transitions, the most striking manifestation of the interference of the orbital and spin currents is the minimum of the $E3$ form factor of the $1d_{5/2} \to 1f_{7/2}$ transition at $q=0.75$ F^{-1}, and, owing to the appearance of this nondiffraction minimum, the small values of the transverse $E3$ form factors compared to the longitudinal $C3$ ones for all the excited states where this transition dominates.

For $1d_{3/2} \to 1f_{7/2}$, $1d_{3/2} \to 1f_{5/2}$, and $1d_{5/2} \to 1f_{5/2}$ transitions the contribution of the orbital current to the $E3$ excitation is small and the structure of the transverse form factor is determined by the contribution of the spin current, and so the $E3$ and $C3$ form factors have similar q dependences. For transitions from the $2s$ shell, contributions of the orbital current to the $E3$ form factor are completely absent.

In Fig. 19a we show the energy distribution of the $E3$ and $M4$ transition strengths for the ^{14}C nucleus (the PCC calculation) near the maxima of the corresponding form factors. Analysis of the q dependences of the form factors of these states found experimentally[30] in backward electron scattering together with the calculated results[25] (Fig. 19b) confirms the assumption that both states have the quantum numbers 3^-, $T=1$.

The energy distribution of octupole isovector resonances in the electroexcitation cross section of light nuclei has not been well studied. This is a consequence of the strong fragmentation of the strengths of these multipole excitations. According to calculations, in $1p$-shell nuclei the intensities of $E3$ resonances are comparable to those of $M4$ resonances, the form factors of which pass through a maximum at

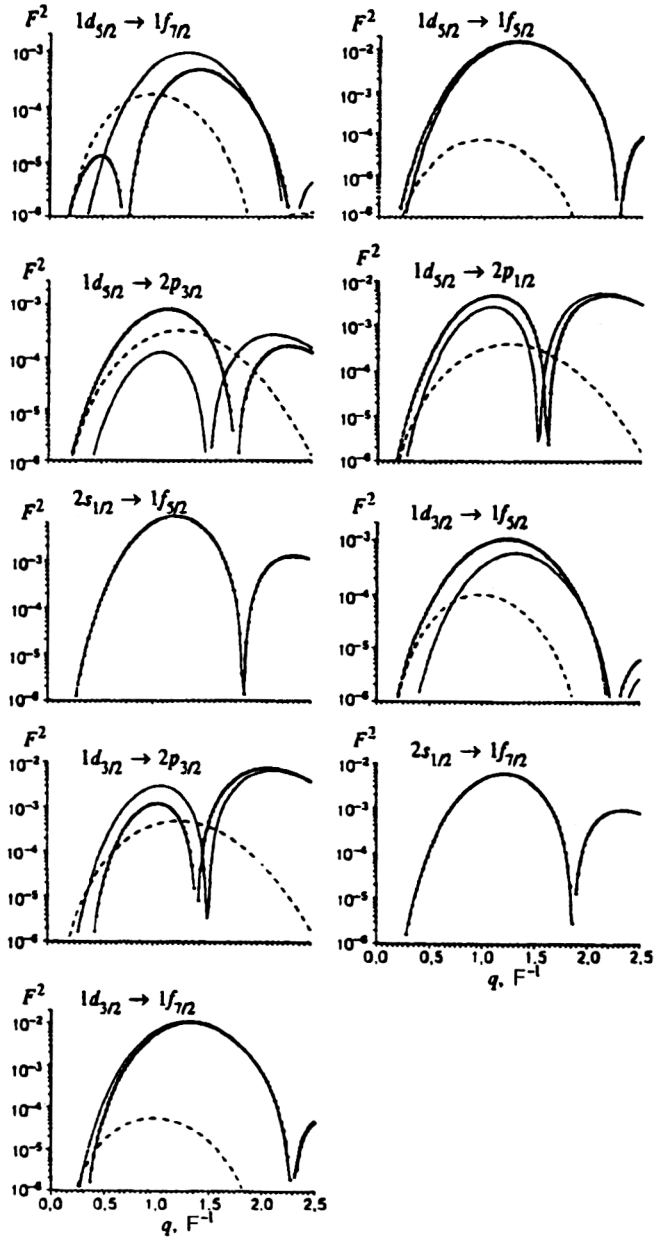

FIG. 18. Squared form factors of single-particle octupole excitations of $1d-2s$-shell nuclei. The notation is the same as in Fig. 17 ($b = 1.85$ F^{-1}).

roughly the same values of the momentum transfer (Figs. 1 and 2). However, the experimentally observed strengths of the individual $E3$ maxima in the electroexcitation cross sections are considerably lower than for $M4$ transitions in the same nuclei. It can be assumed that the interaction of doorway single-particle excitations with more complicated configurations is stronger for $E3$ than for $M4$ resonances. This phenomenon can be partially explained by the higher degree of localization of $E3$ resonances on the energy axis, since the density of states grows with increasing excitation energy. However, the quantitative interpretation of the relative distribution of the strengths of the $E3$ and $M4$ resonances remains an unsolved problem, even for light nuclei.

6. HIGH-SPIN EXCITATIONS OF LIGHT NUCLEI

For $1\hbar\omega$ transitions in light nuclei the maximum multipole order of the excitation is reached at magnetic resonances $MJ_{\max}$. At the level of the doorway excitations these resonances correspond to a unique single-particle transition ($1p_{3/2} \to 1d_{5/2}$ in the $1p$ shell and $1d_{5/2} \to 1f_{7/2}$ in the $1d-2s$ shell). The form factors of states of maximum spin do not contain contributions from the orbital current and are generated by only the spin-octupole nucleon-current operator. The effective excitation cross sections of states with the maximum spin J in reactions involving various probes are functions of the same matrix element of the spin–angular operator $[Y_{J-1} \times \hat{\sigma}]_J$. Therefore, the comparative analysis of $MJ_{\max}$ excitations in reactions involving electrons and hadrons allows nuclear-structure effects to be separated from the dynamics of the interaction between the probe and the nucleus.[8] Finally, the simplicity of the structure of the doorway states and the possibility of extracting spectroscopic information from analysis of the reactions make these excitations a useful object for testing model approximations of nuclear theory.

$M4$ transitions in $1p$-shell nuclei have been studied in the PCC model in Refs. 13, 16 and 17, and in a review.[9] The energy distribution of $M4$ transition strengths obtained in this model for $1p$-shell nuclei has made it possible to explain many of the details of the experimental cross sections. In Fig. 12 we show the dependence of the $M4$ form factor on the momentum transfer for ^{12}C. The HOWF calculation sat-

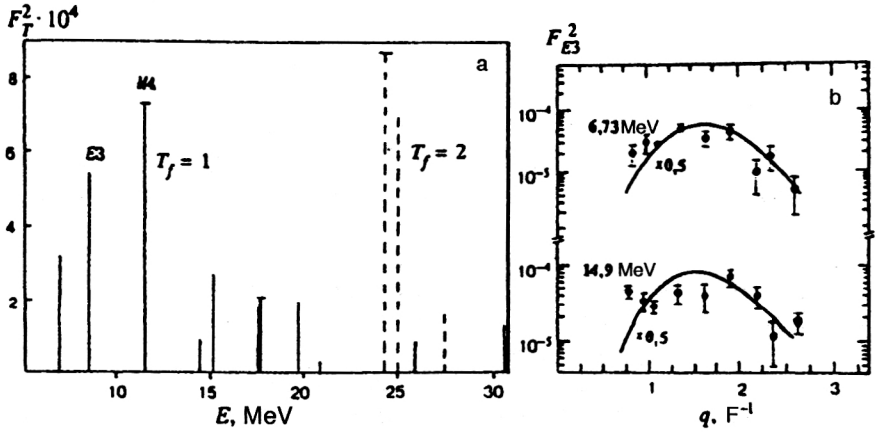

FIG. 19. (a) Energy distribution of the form factors of $E3$ and $M4$ excitations of the ^{14}C nucleus at $q = 1.7$ F^{-1}. (b) Dependence of the form factors of $E3$ excitations of levels of the ^{14}C nucleus on the momentum transfer and the experimental data of Ref. 30.

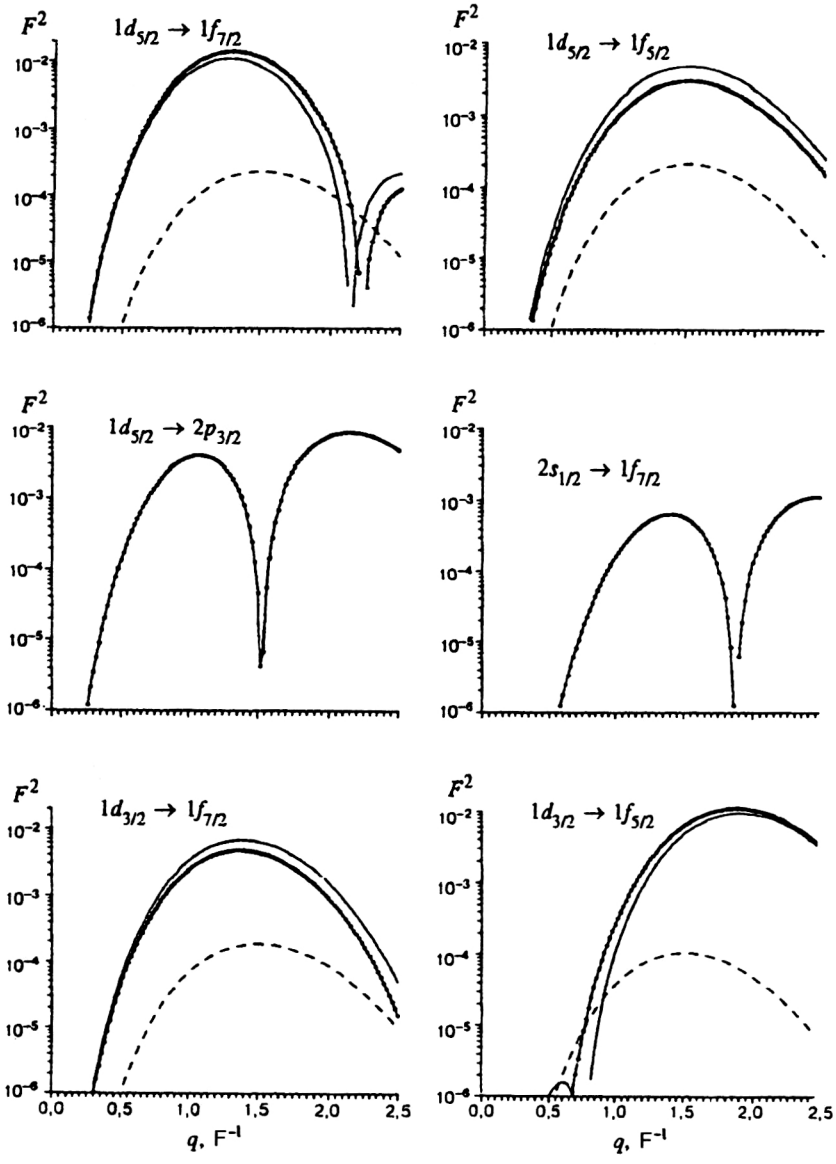

FIG. 20. Squared form factors of single-particle $M4$ transitions in $1d-2s$-shell nuclei. The thin lines are the contributions of the spin currents, and the dashed lines are the contributions of the orbital current. The heavy lines with the points are the $M4$ form factor (calculation with the parameter $b=1.85$ F^{-1}).

isfactorily reproduces the behavior of the experimental form factor for $q<2.5$ F^{-1}.

$M4$ transitions in $1d-2s$-shell nuclei are not pure spin excitations, although the contribution of orbital currents to their form factors is very small (Fig. 20). The contributions of spin currents to these form factors are generated by two spin–angular operators: $[Y_3\times\hat{\sigma}]_4$ ($A3$ in the figures) and $[Y_5\times\hat{\sigma}]_4$ ($A5$). Most of the form factors of $M4$ transitions in $1d-2s$-shell nuclei have maxima in the same range of momentum transfers as the $E5$ and $M6$ form factors (Figs. 21 and 22).[44]

The spin mode $A5$ dominates in the form factors of $E5$ transitions, while the contribution $A3$ is absent. The behavior of the longitudinal $C5$ and transverse $E5$ form factors is similar, and the corresponding curves pass through a maximum at $q=1.8$ F^{-1}, i.e., at the maximum of the $M6$ form factor. The location of this maximum has been reliably determined experimentally.[45] Agreement between the HOWF calculations and the experimental form factor is obtained for the parameter $b=1.85$ F^{-1}, which has been used in all the calculations of the single-particle form factors of $1d-2s$-shell nuclei shown in Figs. 4, 10, and 18, and in the present section.

Therefore, for $1d-2s$-shell nuclei the $M4$, $E5$, and $M6$ excitations have form factors with very similar q dependences, owing to the dominance of the spin mode $A5$ in them. Whereas $E5$ transitions can be identified by studying forward electron scattering, where the $C5$ form factor will be observed in the excitation cross section of the same multipole resonance, distinguishing the $M4$ and $M6$ form factors requires more detailed analysis. Study of $M2$ and $M4$ transitions in the $1p$ shell[42] shows that one way of distinguishing them is by studying the decay properties of the multipole resonance.

The simplicity of the structure of the doorway excitations for $MJ_{\max}$ resonances makes these objects very convenient for studying MR strength fragmentation effects. Recent experiments on $M6$ resonances in $1d-2s$-shell nuclei[45–47] have proved very informative in this regard. For example, comparison of the $M6$ resonances in ^{28}Si and ^{32}S shows how

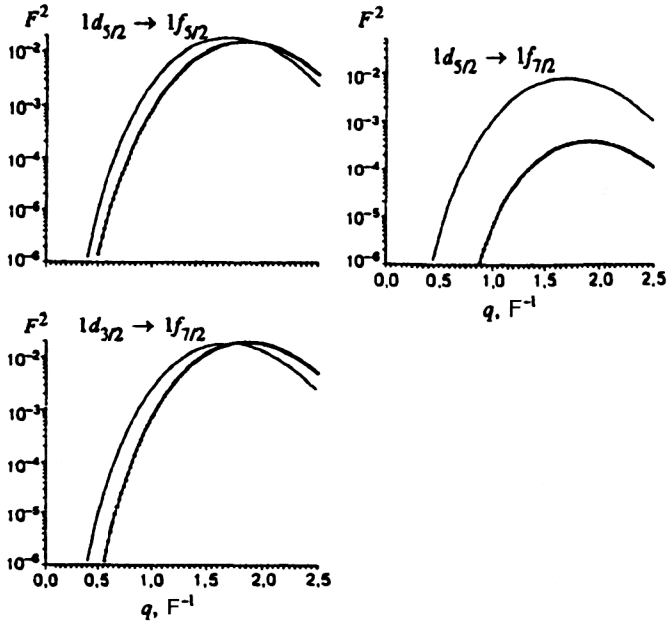

FIG. 21. Squared form factors of single-particle $E5$ transitions in $1d-2s$-shell nuclei. The thin lines are the longitudinal $C5$ form factor, and the heavy lines with the points are the transverse $E5$ form factor. The parameter value $b=1.85$ F^{-1} was used.

important the interaction of the doorway $1d_{5/2} \rightarrow 1f_{7/2}$ excitation with the spectator nucleons of the $2s$ subshell is in the formation of the complicated structure of the $M6$ resonance in ^{32}S.

Finally, it is important to note that studies of $MJ_{\max}$ resonances show that it is possible to interpret the strengths of these transitions quantitatively. Comparison of the experimental results for the total excitation cross sections for states of maximum spin with the theoretical predictions has shown at the preliminary stage that the theoretical predictions are considerably higher than the experimental data. For light nuclei their ratio (the "suppression factor") was about 0.3. The assumption that the nucleon g factors are renormalized in nuclear matter led to much better agreement with experiment: the squared form factor at the maximum was decreased by a factor of two. However, the inclusion of more realistic wave functions of the nuclear ground and excited states significantly reduces the disagreement between theory and experiment[9] even without renormalization of the g factors. This quantitative difference completely vanishes if the matrix elements of single-particle spin-current operators are calculated using nucleon functions in a well of finite depth.[19]

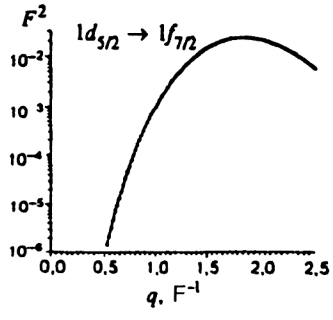

FIG. 22. Squared single-particle form factor of the $M6$ transition. The value $b=1.85$ F^{-1} was used.

CONCLUSION

The main conclusions of our analysis of the form factors of $1\hbar\omega$ excitations of light nuclei and the contribution to them from the orbital and spin components of the nuclear current can be stated as follows:

1. For all multipole resonances there is a characteristic enhancement of the role of the spin components of the intranuclear nucleon current as the momentum transferred to the nucleus increases.

2. The relative contribution of the spin components of the nucleon current to the transverse form factors grows with increasing multipole order of the resonance, reaching 100% for $MJ_{\max}$ transitions.

3. The orbital current determines the behavior of the transverse form factors of electric dipole resonances at small momentum transfers.

4. For a series of single-particle $E1$, $M2$, and $E3$ transitions, destructive interference of the spin and orbital components of the nuclear current leads to the appearance of zeros of nondiffraction origin in the transverse form factors.

5. Comparison of the q dependences of the longitudinal and transverse form factors for electric multipole resonances can serve as a method of identifying the configurational structure of the excited state.

6. The mean energies of resonances whose formation involves several components of the current grow with increasing momentum transferred to the nucleus. This is a consequence of the interplay of the various multipole nuclear-current operators in the transverse form factors.

[1] T. De Forest and J. D. Walecka, Adv. Phys. **215**, 1 (1966).
[2] T. W. Donnelly and J. D. Walecka, Annu. Rev. Nucl. Sci. **225**, 329 (1975).
[3] T. W. Donnelly, Phys. Rev. C **1**, 833 (1970).
[4] M. A. Plum, R. A. Lindgren, J. Dubach *et al.*, Phys. Rev. C **40**, 1861 (1989).

[5]D. G. Ravenhall and D. R. Yennie, Proc. Phys. Soc. London, Sect. A **70**, 857 (1957).
[6]F. Petrovich, R. H. Howell, C. H. Poppe *et al.*, Nucl. Phys. A **383**, 355 (1982).
[7]F. Petrovich, J. A. Carr, and H. McManus, Annu. Rev. Nucl. Sci. **36**, 29 (1986).
[8]R. A. Lindgren and F. Petrovich, *Spin Excitations in Nuclei* (Plenum, New York, 1984), p. 323.
[9]N. G. Goncharova, Fiz. Élem. Chastits At. Yadra **23**, 1715 (1992) [Sov. J. Part. Nucl. **23**, 748 (1992)].
[10]N. G. Goncharova and N. P. Yudin, Phys. Lett. B **29**, 272 (1969); Yad. Fiz. **12**, 725 (1970) [Sov. J. Nucl. Phys. **12**, 392 (1971)].
[11]N. G. Goncharova, Yad. Fiz. **15**, 242 (1972) [Sov. J. Nucl. Phys. **15**, 137 (1972)].
[12]E. N. Goncharova, H. R. Kissener, and Z. A. Éramzhyan, Fiz. Élem. Chastits At. Yadra **16**, 773 (1985) [Sov. J. Part. Nucl. **16**, 337 (1985)].
[13]A. N. Golzov, N. G. Goncharova, and H. R. Kissener, Nucl. Phys. A **462**, 376 (1987).
[14]N. G. Goncharova, A. N. Golzov, and H. R. Kissener, Nucl. Phys. A **462**, 367 (1987).
[15]H. R. Kissener, I. Rotter, and N. G. Goncharova, Fortschr. Phys. **35**, 277 (1987).
[16]N. G. Goncharova, V. J. Spevak, and H. R. Kissener, Nucl. Phys. A **516**, 15 (1990).
[17]N. G. Goncharova, Yad. Fiz. **51**, 1281 (1990) [Sov. J. Nucl. Phys. **51**, 814 (1990)].
[18]R. A. Lindgren, M. Leuschner, B. L. Clausen *et al.*, Can. J. Phys. **65**, 666 (1987).
[19]B. L. Clausen, R. J. Peterson, and R. A. Lindgren, Phys. Rev. C **38**, 589 (1988).
[20]É. R. Arakelyan and N. G. Goncharova, Yad. Fiz. **54**, 920 (1991) [Sov. J. Nucl. Phys. **54**, 557 (1991)].
[21]C. Luettge, P. von Neumann-Cosel, F. Neumeyer *et al.*, Phys. Rev. C **53**, 127 (1996).
[22]R. A. Eramzhyan, M. Gmitro, and H. R. Kissener, Nucl. Phys. A **338**, 436 (1980).
[23]R. A. Eramzhyan and N. G. Goncharova, Z. Phys. A **306**, 89 (1982).
[24]É. R. Arakelyan and N. G. Goncharova, Yad. Fiz. **56**, No. 5, 26 (1993) [Phys. At. Nucl. **56**, 587 (1993)].
[25]É. R. Arakelyan and N. G. Goncharova, Izv. Ross. Akad. Nauk, Ser. Fiz. **58**, 149 (1994) [Bull. Russ. Acad. Sci., Phys. Ser.].
[26]B. S. Ishkhanov, I. M. Kapitonov, V. G. Neudachin, and R. A. Éramzhyan, Fiz. Élem. Chastits At. Yadra **12**, 905 (1981) [Sov. J. Part. Nucl. **12**, 362 (1981)]; R. A. Eramzhyan, B. S. Ishchanov, I. M. Kapitonov, and V. G. Neudachin, Phys. Rep. **136**, 229 (1986).
[27]P. C. K. Kuo, K. G. McNeil, N. K. Sherman *et al.*, Phys. Rev. C **31**, 318 (1985).
[28]D. J. McLean, M. N. Thompson, and D. Zubanov, Phys. Rev. C **41**, 1137 (1991).
[29]R. E. Pywell, B. L. Berman, J. G. Woodworth *et al.*, Phys. Rev. C **32**, 384 (1985).
[30]M. A. Plum, R. A. Lindgren, J. Dubach *et al.*, Phys. Rev. C **40**, 1861 (1989).
[31]A. Yamaguchi, T. Terasawa, K. Nakahara, and Y. Torizuka, Phys. Rev. C **3**, 1750 (1971).
[32]N. G. Goncharova and S. V. Rybkin, Izv. Ross. Akad. Nauk, Ser. Fiz. **61**, 832 (1997) [Bull. Russ. Acad. Sci., Phys. Ser.].
[33]E. R. Arakelyan and N. G. Goncharova, in *Proceedings of the Intern. Nuclear Physics Conf.*, Wiesbaden, 1992, 1.4.34.
[34]E. R. Arakelyan and N. G. Goncharova, Z. Phys. A **348**, 71 (1994).
[35]V. Yu. Ponomarev, V. G. Soloviev, Ch. Stoyanov, and A. I. Vdovin, Nucl. Phys. A **323**, 446 (1979).
[36]N. G. Goncharova, "Microscopic description of multipole excitations of light and intermediate nuclei" [in Russian], Author's abstract of dissertation, Moscow State University, Moscow, 1990.
[37]U. Deutschmann, G. Lahm, R. Neuhausen, and J. C. Bergstrom, Nucl. Phys. A **411**, 337 (1983).
[38]R. S. Hicks, J. B. Flanz, R. A. Lindgren *et al.*, Phys. Rev. C **30**, 1 (1984).
[39]D. J. Millener and D. Kurath, Nucl. Phys. A **255**, 315 (1975).
[40]J. C. Bergstrom, R. Neuhausen, and G. Lahm, Phys. Rev. C **29**, 1168 (1984).
[41]M. A. Plum, R. A. Lindgren, J. Dubach *et al.*, Phys. Rev. C **40**, 1861 (1989).
[42]É. R. Arakelyan and N. G. Goncharova, Yad. Fiz. **59**, 52 (1996) [Phys. At. Nucl. **59**, 47 (1996)].
[43]N. G. Goncharova and A. A. Dzhioev, Vestn. Mosk. Univ. Fiz. Astron. No. 5 (1977) [in press].
[44]N. G. Goncharova and A. A. Dzhioev, *Abstracts of the 48th Meeting on Nuclear Spectroscopy and Nuclear Structure* (Moscow, 1998), pp. 89 and 90.
[45]S. Yen, T. E. Drake, S. Kowalski *et al.*, Phys. Lett. B **289**, 22 (1992).
[46]B. L. Clausen, R. A. Lindgren, M. Farkhondeh *et al.*, Phys. Rev. Lett. **65**, 547 (1990).
[47]B. L. Clausen, R. J. Peterson, C. Kormanyos *et al.*, Phys. Rev. C **48**, 1632 (1993).

Translated by Patricia A. Millard